

CELL EXPANSION DURING DIRECTED DIFFERENTIATION OF STEM CELLS TOWARD THE HEPATIC LINEAGE

Ravali Raju^{1, 3+}, David Chau^{1, 2, 3+}, Dong Seong Cho^{1, 3}, Yonsil Park^{1, 3},
Catherine M Verfaillie⁴, Wei-Shou Hu^{1, 3*}

¹Department of Chemical Engineering and Materials Science, University of Minnesota, Minneapolis, MN 55455-0132, USA

²Department of Biomedical Engineering, University of Minnesota, Minneapolis, MN 55455-0132, USA

³Stem Cell Institute, University of Minnesota, Minneapolis, MN 55455-0132, USA

⁴Department of Development and Regeneration, and Stem Cell Institute Leuven, KU Leuven, Leuven, Belgium

⁺These authors contributed equally to this work

*Corresponding Author

Wei-Shou Hu

Address: 421 Washington Avenue SE

Minneapolis, MN 55455-0132 USA

Phone: (612) 626-7630

Fax: (612) 626-7246

Email: acre@umn.edu

ABSTRACT

The differentiation of human pluripotent stem cells (hPSCs) towards the hepatocyte lineage can potentially provide an unlimited source of functional hepatocytes for transplantation and extracorporeal bioartificial liver applications. It is anticipated that the quantities of cells needed for these applications will be in the order of 10^9 - 10^{10} cells, because of the size of the liver. An ideal differentiation protocol would be to enable directed differentiation to the hepatocyte lineage with simultaneous cell expansion. We introduced a cell expansion stage after the commitment of human embryonic stem cells (hESCs) to the endodermal lineage, to allow for at least an eight-fold increase in cell number, with continuation of cell maturation towards the hepatocyte lineage. The progressive changes in the transcriptome was measured by expression array and the expression dynamics of certain lineage markers was measured by mass cytometry during the differentiation and expansion process. The findings revealed that while cells were expanding they were also capable of progressing in their differentiation towards the hepatocyte lineage. In addition, our transcriptome, protein and functional studies, including albumin secretion, drug-induced *CYP450* expression and urea production, all indicated that the hepatocyte-like cells obtained with or without cell expansion are very similar. This method of simultaneous cell expansion and hepatocyte differentiation should facilitate obtaining large quantities of cells for liver cell applications.

KEYWORDS: EMBRYONIC STEM CELLS, GENOMICS, DIFFERENTIATION, GENE EXPRESSION, HEPATIC

INTRODUCTION

Hepatocytes differentiated from embryonic and induced pluripotent stem cells have the potential of becoming an inexhaustible source of hepatocytes for liver cellular therapies and tissue engineering applications. Stem cell-derived hepatocytes may also be used in bioartificial liver devices to support acute liver failure and drug toxicity screening [1-3]. Over the past decade, several protocols have been established to guide the differentiation of pluripotent stem cells (PSCs) towards the hepatocyte lineage using sequential cocktails of cytokines and growth factors based on our understanding of molecular signals that drive liver development [4-8]. The resulting hepatocyte-like cells (HLCs) express many of the hepatocyte transcripts and exhibit several hepatocyte functions that mimic those of primary hepatocytes [4-9].

One major challenge for future clinical translation of stem cell-derived hepatocytes is to generate a sufficient quantity of cells. Any therapeutic application would require 10^9 - 10^{10} hepatic cells per treatment [10]. To derive HLCs currently, stem cells are expanded to the required quantity before undergoing differentiation towards the hepatocyte lineage. An alternative strategy to circumvent this issue would be to not only expand stem cells in their pluripotent state, but also devise a methodology to expand PSC-derived progeny during their differentiation towards hepatocytes. We hypothesized that with the appropriate signaling cues, it may be possible to expand the number of cells during the process of *in vitro* hepatocyte differentiation by mimicking the native proliferation that occurs naturally *in vivo*.

There have been multiple reports on selective surface markers that could be used for isolation of renewable hepatocyte progenitor cells [11-13]. In one study, hepatocyte progenitor cells were enriched using the surface markers EpCAM or N-cadherin, and subsequently expanded on stromal feeder layers [13]. In addition, a self-renewing endodermal cell line was reported where CXCR4⁺/CD117⁺ cells were sorted and expanded on mouse embryonic feeders [14].

To date, there has not been a report of simultaneous *in vitro* proliferation and differentiation of PSC-progeny, just like *in vivo* fetal liver development. During liver development, cells can undergo extensive proliferation using the signaling cues from their surrounding environment to increase the liver mass. The formation of the endodermal germ layer is among the first differentiation events to occur during mammalian liver development. During gastrulation, signaling through the NODAL protein, a member of the TGFβ family, establishes the distinction between the endoderm and mesoderm germ layers [15,16]. In murine development, the liver along with the lung, pancreas, and stomach are derived from the endoderm around embryonic day E9 of gestation [17,18]. During that period, NODAL protein activates several key transcription factors including *Foxa2* and *Sox17*, that help regulate cell fate commitment to the different endodermal cell lineages [16]. Further signaling cues from the adjacent mesoderm layer are responsible for inducing liver development through fibroblast growth factor (FGF) and bone morphogenetic protein (BMP) signaling pathways [19]. During this stage, hepatocyte progenitor cells arise and proliferate significantly to form the liver bud. Using this knowledge, we attempted to incorporate these native signaling cues to induce further proliferation of differentiating

hepatocyte precursor cells to generate larger numbers of HLCs from the same PSC starting cell number.

In this study, we used growth factor cues to stimulate the native proliferative capacity of definitive endoderm cells while they are differentiating towards the hepatic lineage. We further used a multi-parametric single cell analysis tool [20-22] to examine certain lineage markers to demonstrate that differentiation and proliferation occurred simultaneously in most if not all cells during this process. Using expression arrays and functional studies, we were able to demonstrate that the HLCs generated from expanding definitive endodermal cells were similar to those obtained using the conventional differentiation protocol without the expansion process.

MATERIALS AND METHODS

HUMAN EMBRYONIC STEM CELL CULTURE

The human embryonic stem cell (hESC) line H9 was cultured as described previously [4] using 80% Knockout™ Dulbecco's modified Eagle medium (DMEM) (Gibco/BRL), supplemented with 20% Knockout Serum Replacement (Gibco, USA), 2.0 mM glutamine, 1X nonessential amino acids (Gibco, USA), 55 μ M β -mercaptoethanol and basic fibroblast growth factor (FGF2, R&D) (10 ng/mL). The cells were cultured on irradiated E13-E14 CF-1 mouse embryonic fibroblasts (MEFs) (Charles River Laboratories, Wilmington, MA), at 37°C in 10% CO₂. The cells were passaged on a regular basis every 2-3 days using 0.1% (w/v) Collagenase Type IV (Gibco) in Knockout™ DMEM after reaching ~50-70% confluency.

HEPATOCYTE DIFFERENTIATION

H9 cells were plated in 12 well plates coated with 2% Matrigel® (BD Biosciences) in mTESR™ medium (Stem Cell Technologies) for 24 hours or until confluency was reached. Differentiation was initiated by switching to differentiation medium consisting of a 60/40 (v/v) mixture of low glucose Dulbecco's Modified Eagle media (DMEM) (Gibco, USA) and MCDB-201 (Sigma), supplemented with 26 µg/mL ascorbic acid 3-phosphate (Sigma), linoleic acid and bovine serum albumin (LA-BSA, Sigma) (0.25 mg/mL BSA and 2.35 µg/mL linoleic acid), insulin-transferrin-selenium (ITS, Sigma) (2.5 µg/mL insulin, 1.38 µg/mL transferrin, 1.25 ng/mL sodium selenite), 0.4 µg/mL dexamethasone (Sigma), 4.3 µg/mL β-mercaptoethanol (Hyclone), 100 IU/mL penicillin and 100 µg/ml streptomycin (Gibco, USA) . 2% fetal bovine serum was added to the media (v/v) in Stage I for the first six days and 0.5 % (v/v) for the remaining period.

The differentiation medium was supplemented with stage specific growth factors: Stage 1, Activin A (100 ng/ml) and Wnt3a (50 ng/ml); Stage 2, FGF2 (10 ng/ml) and BMP4 (50 ng/ml); Stage 3, FGF8b (25 ng/ml), FGF1 (50 ng/ml) and FGF4 (10 ng/ml); Stage 4, HGF (20 ng/ml) and Follistatin (100 ng/ml) (Figure 1a). Differentiations were carried out at 21% O₂ and 5% CO₂ with a 50% media change every 2 days during differentiation. A complete media change was performed when changing the stages of differentiation (i.e. day 6, 10, and 14).

For endodermal cell expansion, cells were harvested on Day 6 after the initiation of hepatocyte differentiation using 0.1% (w/v) Collagenase Type IV (Gibco) in Knockout™ DMEM and plated onto Matrigel® pre-coated plates in Stage 2 medium containing FGF2 (10 ng/ml) and BMP4 (50

ng/ml). A day after plating, the media was completely replenished with Stage 2 medium to remove any unattached cells. On the 3rd day after plating, the cells were passaged again using 0.1% (w/v) Collagenase Type IV onto Matrigel® coated plates in Stage 2 medium. Three days after the second passaging the medium was changed to Stage 3 medium to continue the differentiation.

QUANTITATIVE REAL TIME POLYMERASE CHAIN REACTION (QRT-PCR)

Total RNA was obtained from cell lysates using the RNeasy Micro Kit (Qiagen). cDNA was synthesized using the Superscript III reverse transcriptase kit (Invitrogen) according to manufacturer's instructions. Transcript abundance levels of a sample were normalized to the housekeeping gene, *GAPDH*. Sequences for the primers of the genes used in this study are listed in Table S1. For comparison among cells at different stages of differentiation, these values were then normalized to hESCs and expressed as \log_{10} (Expression level relative to hESC).

IMMUNOHISTOCHEMISTRY

The cells were fixed with 4% paraformaldehyde at room temperature for 20 min, then blocked with PBS containing 0.2% Triton-X-100 and 1% donkey serum or BSA (Sigma) at room temperature for 1 hr. After blocking, samples were incubated with primary antibodies AFP (Dako, 1:1000), ALB (Dako 1:1000), SOX17 (R&D, 1:20), FOXA2 (Abcam, 1:1000) and DAPI (Life Technologies, 1:500) overnight at 4 °C. The cells were then incubated with secondary antibodies (anti-mouse IgG1 Alexa Fluor 488 labeled (Molecular Probes, 1:500 dilution), anti-rabbit IgG Alexa Fluor 488 (Molecular Probes, 1:500 dilution), or anti-mouse IgG Alexa Fluor 555 (Molecular Probes, 1:500 dilution)) for 30 min at room temperature. Negative controls were cells incubated with only the relevant isotype control and secondary antibody.

MASS CYTOMETRY

Lyophilized antibodies for FOXA2, SOX17, ALB, DLK1, AFP, and AAT proteins were obtained from R&D systems. 200 µg of antibodies were conjugated with a selected panel of heavy metal isotopes using the MaxPar® antibody labeling kit from Fluidigm according to the manufacturer's instructions with slight modifications. The antibodies were eluted in 50 µl PBS instead of W buffer provided by the kit to improve antibody recovery. The conjugated antibodies were diluted to 0.5 mg/mL in antibody stabilizer solution (Candor Biosciences, 131050) and stored at 4 °C until use. Metal conjugated CXCR4 and CD44 were directly obtained from DVS Sciences (Sunnyvale, CA).

Cells were collected with 0.1% collagenase in DMEM and dissociated into single cells using trypsin as previously described [5]. About 500,000 cells per sample were fixed using 10 % formalin for 20 min at room temperature. The cells were washed with PBS and centrifuged before being resuspended in 5 µL Human TruStain FcX™ (BioLegend, 422302) and 95 µL PBS at room temperature for 10 min for blocking. The cells were first incubated in a cocktail of metal conjugated antibodies targeting surface markers in 100 µl of PBS for 30 min at room temperature. Cells were washed twice with PBS and incubated with a second cocktail of antibodies targeting intracellular proteins suspended in 100 µL SAP buffer (PBS with 0.1% (w/v) saponin (Sigma, 47036) and 0.05% (w/v) sodium azide (Sigma, 438456)) for 30 min at room temperature. After washing twice with SAP buffer, cells were incubated with MaxPar® Intercalator-Ir 125 µM (DVS Sciences, 201192A) at a dilution of 1:1000 in 1 mL of SAP buffer

overnight at 4°C. Cells were washed twice, suspended in 500 µL water and passed through a cell strainer and analyzed on the CyTOF2 instrument (DVS Sciences). Serially diluted antibodies in an antibody cocktail were used to titrate the antibody concentration using hESCs as a negative control (Data not shown). Data was analyzed using the Cytobank software (Fluidigm) and visualized in Spotfire (Tibco). Data from mass cytometry was visualized and analyzed using a flow cytometry experiment data processing software (FlowJo™). A metal-encoded DNA intercalator (i.e. Ir191 and Ir193) was used to label nucleated cells [20]. Samples from different time points were normalized to each other by assigning the same DNA intercalator median intensity value for each sample. Events with very low (intercalator reading <20) or very high (intercalator reading > 5000) intensity were removed to exclude cell debris or cell aggregates. The filtered events were further analyzed using a spanning-tree progression analysis of density-normalized events (SPADE) from Cytobank [20,23].

FUNCTIONAL ANALYSIS OF HLCS

Albumin was measured using a human specific albumin ELISA kit (Starters Kit Bethyl E101 and Bethyl E80-129). Urea was measured using the QuantiChrom Urea Assay Kit (BioAssay Systems). Periodic-Acid-Schiff staining (Sigma-Aldrich) was performed according to the manufacturer's protocol. The cells were immersed in Periodic Acid solution for 5 min and in Schiff's reagent for 15 min at room temperature followed by a wash with DI water. To test the function of CYP450 enzymes, cells were incubated for 24 hours in differentiation media with or without 50 µM rifampicin (Gold Biotechnology). The transcript levels of *CYP2A6*, *CYP2C8* and *CYP2C9*, were measured using qRT-PCR.

TRANSCRIPTOME ANALYSIS

Total RNA was extracted from cell samples at various time points of differentiation using the RNeasy Mini kit (Qiagen). The transcriptome assay using the Illumina HT12 bead array v3 (Illumina Inc) was performed by the University of Minnesota Genomic Center (UMGC).

Data was processed using the *lumi* package in R [24]. Transcriptome data from 34,000 probes representing about 20,000 genes was obtained. Principal component analysis (PCA) was performed in R. Spotfire (Tibco) and a MATLAB script TimeView were used for data visualization and functional analysis [25].

RESULTS

EXPANSION OF ENDODERMAL CELLS

hESCs were differentiated to definitive endoderm (DE) in Stage 1 using a medium containing Activin and Wnt3a to reach cell densities of 2.5×10^5 cells/cm² in six days (D6). The cells were then detached by 0.1% collagenase treatment and passaged at $\sim 6 \times 10^4$ cells/cm² onto Matrigel® coated plates in Stage 2 medium containing FGF2 and BMP4 (Figure 1a). Cells adhered to the surface a few hours after plating, and expanded up to 3-fold in viable cell number after three days (Figure 1b and S1; Endoderm 1, EN1). Cells were then passaged again in Stage 2 medium containing FGF2 and BMP4, that have been reported to provide the necessary proliferative cues to endodermal cells during embryonic liver development [26]. The endodermal cell population expanded approximately 8-fold after two passages as shown in Figure 1b (Endoderm 2, EN2). Further passages beyond the second passage were carried out, resulting in cell expansion up to

15 fold; however, we detected an increasing population of cells with a fibroblastic morphology (Data not shown). By contrast, when we tracked the cell expansion during Stage 2 of the conventional differentiation method without passaging, we observed that the cell expansion was limited only up to two-fold (Figure 1b). Thus, by implementing two passaging steps during the hepatic endoderm commitment stage, we were able to induce an 8-fold expansion by providing additional surface area with the signaling cues of Stage 2 medium.

EXPRESSION OF HEPATOCYTE GENES AND PROTEINS IN EXPANDED ENDODERMAL CELLS

We evaluated the expression of pluripotency, endoderm and hepatic endoderm related genes in cells during the expansion by qRT-PCR and immunostaining. Expression of Octamer-binding transcription factor 4 (*OCT4*), a master regulator of the pluripotency network in hESCs [27], decreased about 1000 fold during the course of endodermal expansion as expected (Figure 2a). The endodermal transcription factor, goosecoid homeobox (*GSC*), a key marker for differentiating definitive and visceral endoderm [28], and *CXCR4*, a surface marker co-expressed with *GSC* [28], were both highly expressed in the D6 population but decreased in the EN1 and EN2 populations. (Figure 2a). Our hypothesis was that similar to *in vivo* development, ESC-derived definitive endoderm cells, can proliferate while at the same time differentiate to hepatic endoderm. We also evaluated the expression of the genes indicative of maturation to hepatic committed endoderm and hepatoblasts. In line with our hypothesis, the decrease in definitive endoderm marker gene transcripts was accompanied by almost 1000 fold increase of the transcript level of alpha-fetoprotein (*AFP*) and albumin (*ALB*) over the expansion period [29]. These dynamics of gene expression suggest the gradual transition of an endodermal-committed phenotype towards a more hepatic phenotype during the expansion process.

We also compared the transcript levels of hepatic endoderm/hepatoblast genes in the EN1 and EN2 populations to cells obtained at the end of Stage 2 (D10) and Stage 3 (D14) from the conventional differentiation process without cell expansion. Expression levels of *OCT4*, *CXCR4*, and *GSC* in EN1 and EN2 cells were similar to those in D10 and D14 cells, respectively (Figure 2a). Levels of the hepatic transcripts, *AFP* and *ALB*, increased more gradually in the conventional method of differentiation (D10 and D14), compared to cells undergoing cell expansion (Figure 2a).

The transition from an endoderm to a more hepatic stage was also examined by immunostaining (Figure 2b and S2). Forkhead Box A2 (FOXA2) and SRY (Sex determining Region Y)-Box 17 (SOX17), key transcription factors in the establishment of definitive endoderm, were prominent in the D6 stage but diminished by the EN2 and D14 stage. In contrast, AFP was absent in the D6 stage, and became more prominent in both the EN2 and D14 population consistent with the transcript levels observed. The results suggest that cells undergoing expansion are differentiating simultaneously.

CHARACTERIZATION OF DIFFERENTIATION/EXPANSION PROCESS BY MASS CYTOMETRY

To identify whether the increase in transcript for hepatic endoderm/hepatoblast marker genes and proteins during expansion was restricted to a differentiated subpopulation of cells, or was occurring in most of the population, we used mass cytometry to examine co-expression of a panel of endodermal and hepatic markers at a single cell resolution [20]. Cells undergoing

differentiation were labeled with stable isotopes of lanthanide heavy metal conjugated with antibodies against endodermal marker proteins (CXCR4, FOXA2, SOX17) and hepatic marker proteins (DLK1, CD44, AFP, ALB and AAT). Similar to flow cytometry, the antibody labelled-cells were sorted into single cells. But instead of detecting various fluorescent tags, the sorted cells are vaporized to leave the stable isotope tags to be analyzed by a time of flight (TOF) mass spectrometry. In the TOF analysis, different antibody tags will give sharp and distinctive signatures corresponding to its conjugated metal isotope, allowing for quantification of each labelled antibody without the need of resolving spectrum spillover or overcoming autofluorescence that normally occurs in multiple parametric flow cytometry.

Due to the complexity of the many markers that was used to label a particular cell, 3-D diagrams were used to efficiently plot the different marker expression levels. During the course of differentiation, various combinations of marker expressions were plotted as 3-D diagrams with three markers represented along the X, Y, Z axes and CD44 represented as a color gradient as shown in Figures S3 and S4. Still, with such plots it is not easy to gain a global view of the evolution of the population during the directed differentiation. Thus, we used the expression level of all 8 markers to characterize the co-expression in the different populations using Spanning-tree Progression Analysis of Density-normalized Events (SPADE) which groups the cells into a defined number of clusters based on its expression pattern [23].

The SPADE analysis utilizes a combined dataset that consists of all the markers' expression level for cells of different differentiation stage during directed differentiation. The dataset was then

clustered into 75 nodes based on the expression level of the eight markers for each cell, and the clustering results are shown as a tree diagram (Figure S5). Each node constitutes a cluster of cells with a similar pattern of expression for all eight markers. Because eight markers are used, eight tree diagrams are used to present the results for each marker (Figure S5).

Based on the expression pattern of the different lineage specific markers, certain nodes can then be assigned to one of three subpopulations: (A) endodermal cells, (B) hepatic endoderm/hepatoblasts, and (C) hepatoblasts/hepatocytes (Figure S5a-h). The designation of the different subpopulation is based on the expression pattern of the different markers and is described more in detail in the legend of Figure S5. The nodes of the same subpopulation are encircled in a dashed line. However, not all nodes were assigned to a subpopulation, especially those with low expression levels of most markers.

To validate our classification of the nodes into the different subpopulations, we performed k-means clustering on the 75 nodes using the median intensity of each marker for each node. The vast majority of the nodes for subpopulations A (endodermal cells) and C (hepatoblast/hepatocytes) were assigned to its own distinct clusters. The majority of nodes in subpopulation B (hepatic endoderm/hepatoblasts) were mainly scattered across the two clusters (Figure S5i). The results of the k-means clustering illustrated that the majority of the nodes within a subpopulation were grouped to the same clusters supporting our classification of the 75 nodes into 3 subpopulations.

The mass cytometry data for each stage of differentiation was then mapped to the previously made SPADE tree diagram to illustrate the heterogeneity of the different subpopulations within each stage. The fraction of cells that were classified to a node for a particular stage will then be illustrated by the size and color of the node (Figure 3). Using the fraction of cells for each subpopulation, we can then quantitatively determine the heterogeneity at each stage of the differentiation/expansion. On D6, 51% of the cells were definitive endodermal cells, expressing CXCR4, SOX17, or FOXA2. During the expansion stage (EN1 and EN2) the definitive endodermal cells decreased to less than 10% while the early hepatic endoderm/hepatoblasts increased steadily to over 50%. The decrease of definitive endodermal cells and increase of hepatic endoderm/hepatoblasts was similar to what we observed in cultures without expansion (from D6 to D14). At the end of the directed differentiation, a similar percentage of hepatocyte-like cells was obtained with cell expansion (75%) or without (76%). However, considering that the cell number had increased significantly at the EN2 stage as compared to D14 of differentiation, the total number of hepatocytes obtained is substantially higher with cell expansion.

We also used immunostaining to examine key differentiation markers (costaining of AFP and ALB, or FOXA2 and SOX17) to confirm the results of mass cytometry measurements. The percentage of cells that were positive for those markers were compared to that obtained using mass cytometry for different populations (Figure S6). Images of multiple microscopic fields for each population sample were randomly taken and the number of all nucleated cells and fluorescently stained cells were quantified using CellProfiler [30]. Some differences were

observed between the percentage of cells stained and percentage through mass cytometry. However, these small differences in percentages between the two approaches were likely caused by the chosen threshold values of mass cytometry data classifying positive and negative cells. Nevertheless, the overall trend of the dynamics of marker expression was still the same in both of the immunostaining and mass cytometry results.

DIFFERENTIATION POTENTIAL AND FUNCTIONAL ACTIVITY OF EXPANDED ENDODERMAL CELLS

The results of the mass cytometry studies suggested that the majority of the expanded cells (EN2) were capable of differentiating to HLCs. To confirm that HLCs derived with or without cell expansion were of the hepatic phenotype, both populations were immunostained and shown to be positive for the hepatic marker, ALB (Figure 2c). We evaluated the transcript level of key hepatocyte marker genes in D20-HLCs and in EN2-HLCs, including phosphoenolpyruvate carboxykinase (*PEPCK*), alpha-1 antitrypsin (*AAT*), *AFP* and *ALB*. The EN2-HLC population expressed all the hepatocyte transcripts levels 10^2 - 10^5 higher compared to hESC, similar to D20-HLCs (Figure 4a). Transcripts of a number of cytochrome P450 enzymes were also expressed. Drug exposure to hepatocytes often induces specific CYP450 enzymes involved in its metabolism. Following exposure to rifampicin, we could detect increased transcript levels of its corresponding CYP450 enzymes (*CYP2C8*, *CYP2C9* and *CYP2A6*) in D20-HLCs and EN2-HLCs (Figure 4b) [31]. The level of increase was comparable between EN2-HLCs and D20-HLCs.

In addition to drug metabolism, albumin synthesis and urea secretion for both D20-HLC and EN2-HLC populations were also measured and shown to be comparable (Figure 4c-d) [5].

Glycogen synthesis was evident in both D20-HLC and EN2-HLC cells as assessed by PAS staining (Figure 4e).

COMPARATIVE TRANSCRIPTOME ANALYSIS OF CELLS FROM THE ORIGINAL AND MODIFIED PROTOCOL

The transcriptome of cells at different stages of directed differentiation were evaluated and subjected to PCA. The first two principal components (PCs) representing 90% of the variance among all samples were chosen to plot all the samples in a two-dimensional PC space as shown in Figure 5. ESC, D6, D10, D14 and D20-HLC lined up chronically in order according to their differentiation stages, with the least and most mature cells on the two separate ends of the plot. EN1, EN2 and D10 cells, all exposed to Stage 2 medium, cluster in a similar region, with EN1 and EN2 lying between D6 and D10 cells. Both EN2-HLC and D20-HLC co-localize in the same region, almost overlapping one another, confirming their similarity in spite of the differences with respect to cell expansion.

The gene expression dynamics of cells undergoing directed differentiation from both protocols were compared and plotted in groups of similar functional classes (Figures 7 and S7-S8). Overall the gene expression profiles show that, regardless of whether or not cells were expanded during the endodermal stage, their gene expression dynamics were very similar. The transcript level of pluripotent genes *POU5F1*, *NANOG*, *SOX2*, *ZIC3*, *SALL4*, and *LIN28* decreased from the beginning of differentiation as expected (Figure S7). Endodermal genes *EOMES*, *CXCR4*, *GSC*, and *SOX17* increased in the first stage of differentiation, then decreased in the following stages either accompanied by cell expansion or not (Figure 6a). In the presence of Stage 2 medium, a

gradual increase in the transcripts of hepatoblast and hepatic genes is seen during the course of differentiation, including transcripts for *AFP*, *DLK1*, *TTR*, and *KRT8* (hepatoblast specific markers) as well as *ALB*, *PEPCK*, *PCK2*, transferrin (*TF*), α_1 -antitrypsin (*AIAT*) (more mature hepatocyte markers) (Figure 6b and S8). The expression level of genes pertaining to important liver functions such as glycolysis/gluconeogenesis, urea cycle, fatty acid metabolism, and drug detoxification were also similar in D20-HLCs and EN2-HLCs (Figure S9). The similarity in transcript levels of these genes gives further credence to the notion that although the endodermal cells underwent expansion, they retained undiminished differentiation capability to HLCs to a degree similar to that of unexpanded endodermal cells.

DISCUSSION

The differentiation of PSCs towards the hepatocyte lineage raises the possibility of having an unlimited supply of human hepatocytes for a number of cellular applications [4,6-8]. Although all protocols vary somewhat, they typically consist of treating stem cells with a combination of growth factors/cytokines in stages to mimic the key signaling cues occurring during embryonic development. However, cellular proliferation, which is integral during *in vivo* development, is typically absent or minimal in directed differentiations of stem cells to hepatocytes. In this study, we purposefully introduced cell expansion during the differentiation process between the time of commitment to definitive endoderm and the time hepatic endoderm/hepatoblasts are being generated, with a goal to not only generate larger quantities of HLCs but also to more accurately mimic *in vivo* development where expansion also occurs.

In this study, we demonstrated that hESCs, during the course of hepatocyte differentiation, could be expanded at an intermediate endodermal stage and continued to differentiate towards a hepatocyte-like phenotype. To mimic the proliferative capability of developing hepatic cells, we utilized the soluble factors known to induce endoderm differentiation and promote proliferation as a way to incorporate an expansion stage. The factors, BMP4 and FGF2, were chosen to mimic the signaling of the cardiogenic mesoderm and septum transversum mesenchyme during the transition of the foregut endoderm to the liver bud, a process that involves extensive cell migration, proliferation and differentiation [17]. By providing more surface area to cells at the intermediate endodermal stage, cells demonstrated the ability to expand up to at least 8-fold. Given that we split the cells at a ratio of 1:4 during the first passage, the initial EN population showed remarkable proliferative capability within 3 days. By the third passage, up to 15-fold increase in cell number was occasionally achieved but the resulting expansion from the third passage of cell expansion was not as consistent. In addition, cells with a fibroblastic morphology began to emerge when cells were passaged beyond the second expansion stage, suggesting that the expanding endodermal cells have a limited proliferative capability similar to developing cells *in vivo*. However, the increase in cell number during the expansion demonstrated that stem cell derived endodermal cells exhibit a proliferative capability also seen with endodermal cells in developing embryos [17-19]. The expansion in cell number was also accompanied by a simultaneous increase in hepatocyte transcript levels along with a drastic decrease in endodermal and pluripotent marker gene expression (Figure 2). This finding correlates with what happens to developing endodermal cells undergoing proliferation as they commit to the different endoderm lineages during liver development [17].

Our results indicated that the definitive endoderm cells were capable of simultaneous proliferation and differentiation. However, it is not clear whether the changes in gene expression happen to a larger population of cells or to only a small population. We employed mass cytometry to examine the progression of cells at different stages of differentiation. The population of cells at different stages was further classified into different subpopulations to examine the dynamics of the cells during differentiation. In the D6, EN1, EN2, and D14 populations, only 50-75% of the population were categorized as either endodermal cells, hepatic endoderm/hepatoblasts, or hepatoblasts/hepatocytes. But by the end of the differentiation, the percentage of hepatic-committed cells had increased to almost >90%. These results suggest that cells differentiate at different rates; giving rise to a heterogeneous population at different stages of differentiation. It is noted that a large number of the nodes in the SPADE tree were not included as the different classes of differentiated cells. Although the density of cells in each of those nodes was small, altogether they constitute a significant fraction of the total cells. It is likely that those cells are in a transition stage and also possible that they might include some cells that failed to differentiate towards the hepatic lineage. Nevertheless, the majority of the population is differentiating along the hepatic lineage. The decrease in endodermal and increase in hepatocyte markers occurred in a majority of the cells, as a large fraction of the population co-expressed multiple hepatocyte markers and lost the expression of early stage markers simultaneously. Furthermore, the results demonstrate that the increased hepatic transcript level in EN2-HLC was not merely caused by a small subset of cells expressing extremely high levels of hepatocyte markers, but was attributed by a majority (>75%) of the cells differentiating towards

the hepatic lineage. Moreover, these novel quantitative analyses of the differentiation of endodermal cells confirmed that the majority of cells following the expansion process were also capable of becoming HLCs. Indeed, the resulting EN2-HLC population was similar to D20-HLC: both containing a large fraction of cells expressing moderate to high levels of ALB, AFP, AAT and CD44, but low levels of endodermal markers. The similarity between EN2-HLC and D20-HLC was further confirmed by their ability to secrete albumin, synthesize urea and induce cytochrome P450 enzymes in response to rifampicin.

Mass cytometry have been used to explore the heterogeneity in the hematopoietic system and in cancer [20,23,32-36]. In stem cell research, it has been used to explore the emergence of induced pluripotent stem cells from fibroblasts [37]. In this study, we employed mass cytometry to examine the population dynamics during directed differentiation of stem cells toward the hepatic lineage. Importantly, we took advantage of the detailed analysis at the single cell level provided by mass cytometry by imposing quantitative criteria for each marker to perform quantitative analysis of the emergence of different subpopulations at different stages of differentiation. The mass cytometry data demonstrate that while endodermal cells underwent expansion, they continued on the trajectory of differentiation toward the hepatocyte lineage (Figure 3). This was further supported through microarray analyses. Using PCA on the transcriptome data, we plotted the results on a PC1 vs. PC2 space to demonstrate the similarities between each sample (Figure 5). All cell samples lined up in the order of their progression towards the hepatocyte lineage. EN1 and EN2 were positioned in between D6 and D10 cells, suggesting that their differentiation status is more advanced than D6 but not as mature as D10. Thus, during expansion, endodermal

cells were proliferating while also differentiating towards a more hepatic endoderm/hepatoblast fate instead of remaining in a renewable endoderm cell stage [14].

In this study, hESCs were simultaneously expanded while differentiating towards hepatic lineage. Other studies have reported the expansion of hepatocyte progenitor cells [12-14]. By FACS sorting, EpCAM⁺/c-KIT⁻ hepatic progenitor cells from differentiating mouse ESCs were isolated and subsequently expanded on mouse embryonic feeders [12]. In another study, human hepatoblasts were sorted from ESC progeny based on N-cadherin expression (14), and subsequently cultured as progenitors on stromal feeder cells. Human endodermal progenitor cells have also been clonally isolated from a differentiating population based on expression of the surface markers CXCR4 and CD117, and expanded on Matrigel® and feeder cells. These progenitor cells were subsequently differentiated to express hepatic markers. In all three studies the cells were maintained at a “progenitor” state and did not appear to continue to differentiate until they were removed from the feeder and exposed to hepatocyte differentiation conditions. By contrast, in our study, the bulk of the starting population was expanded and differentiated simultaneously, mimicking embryonic liver development in which hepatic endoderm and early hepatoblast differentiation occurs while the size of the liver is rapidly increasing.

In spite of the increased expression of a number of hepatic genes, both D20-HLCs and EN2-HLCs are not yet mature hepatocytes as transcript levels of enzymes involved in xenobiotic biotransformation are significantly lower in HLCs than in neonatal or adult hepatocytes (Data not shown). In addition, the degree of cell expansion achieved in this study is still limited. For

potential applications in the future, a substantially larger level of expansion will still be more desirable. Further improvement of the protocol for hepatocyte differentiation from pluripotent stem cells is necessary to extend cell expansion and to achieve maturity of HLCs. However, our findings indicate that it is possible to expand endodermal cells during hepatocyte differentiation, which might alleviate the time and effort in generating large quantities of HLCs.

ACKNOWLEDGEMENTS

David Chau was supported by the NIH Biotechnology Training Grant (GM08347). The CMV group was supported by FWO-G067314N, IWT-SBO-HILIM-3D, EC-SEURAT-1-HEMIBIO.

Disclosure Statement

No competing financial interests exist.

REFERENCES

1. Haridass D, N Narain and M Ott. (2008). Hepatocyte transplantation: waiting for stem cells. *Curr Opin Organ Transplant* 13:627-32.
2. Hughes RD, RR Mitry and A Dhawan. (2012). Current status of hepatocyte transplantation. *Transplantation* 93:342-7.

3. Raju R, D Chau, CM Verfaillie and WS Hu. (2013). The road to regenerative liver therapies: the triumphs, trials and tribulations. *Biotechnol Adv* 31:1085-93.
4. Roelandt P, KA Pauwelyn, P Sancho-Bru, K Subramanian, B Bose, L Ordovas, K Vanuytsel, M Geraerts, M Firpo, R De Vos, J Fevery, F Nevens, WS Hu and CM Verfaillie. (2010). Human embryonic and rat adult stem cells with primitive endoderm-like phenotype can be fated to definitive endoderm, and finally hepatocyte-like cells. *PLoS One* 5:e12101.
5. Subramanian K, DJ Owens, R Raju, M Firpo, TD O'Brien, CM Verfaillie and WS Hu. (2014). Spheroid culture for enhanced differentiation of human embryonic stem cells to hepatocyte-like cells. *Stem Cells Dev* 23:124-31.
6. Basma H, A Soto-Gutierrez, GR Yannam, L Liu, R Ito, T Yamamoto, E Ellis, SD Carson, S Sato, Y Chen, D Muirhead, N Navarro-Alvarez, RJ Wong, J Roy-Chowdhury, JL Platt, DF Mercer, JD Miller, SC Strom, N Kobayashi and IJ Fox. (2009). Differentiation and transplantation of human embryonic stem cell-derived hepatocytes. *Gastroenterology* 136:990-9.
7. Si-Tayeb K, FK Noto, M Nagaoka, J Li, MA Battle, C Duris, PE North, S Dalton and SA Duncan. (2010). Highly efficient generation of human hepatocyte-like cells from induced pluripotent stem cells. *Hepatology* 51:297-305.
8. Yu Y, H Liu, Y Ikeda, BP Amiot, P Rinaldo, SA Duncan and SL Nyberg. (2012). Hepatocyte-like cells differentiated from human induced pluripotent stem cells: relevance to cellular therapies. *Stem Cell Res* 9:196-207.

9. Li T, J Huang, Y Jiang, Y Zeng, F He, MQ Zhang, Z Han and X Zhang. (2009). Multi-stage analysis of gene expression and transcription regulation in C57/B6 mouse liver development. *Genomics* 93:235-42.
10. Sharma S, R Raju, S Sui and WS Hu. (2011). Stem cell culture engineering - process scale up and beyond. *Biotechnol J* 6:1317-29.
11. Sharma AD, T Cantz, A Vogel, A Schambach, D Haridass, M Iken, M Bleidissel, MP Manns, HR Scholer and M Ott. (2008). Murine embryonic stem cell-derived hepatic progenitor cells engraft in recipient livers with limited capacity of liver tissue formation. *Cell Transplant* 17:313-23.
12. Li F, P Liu, C Liu, D Xiang, L Deng, W Li, K Wangenstein, J Song, Y Ma, L Hui, L Wei, L Li, X Ding, Y Hu, Z He and X Wang. (2010). Hepatoblast-like progenitor cells derived from embryonic stem cells can repopulate livers of mice. *Gastroenterology* 139:2158-2169 e8.
13. Zhao D, S Chen, J Cai, Y Guo, Z Song, J Che, C Liu, C Wu, M Ding and H Deng. (2009). Derivation and characterization of hepatic progenitor cells from human embryonic stem cells. *PLoS One* 4:e6468.
14. Cheng X, L Ying, L Lu, AM Galvao, JA Mills, HC Lin, DN Kotton, SS Shen, MC Nostro, JK Choi, MJ Weiss, DL French and P Gadue. (2012). Self-renewing endodermal progenitor lines generated from human pluripotent stem cells. *Cell Stem Cell* 10:371-84.
15. David NB and FM Rosa. (2001). Cell autonomous commitment to an endodermal fate and behaviour by activation of Nodal signalling. *Development* 128:3937-47.

16. Kim SW, SJ Yoon, E Chuong, C Oyolu, AE Wills, R Gupta and J Baker. (2011). Chromatin and transcriptional signatures for Nodal signaling during endoderm formation in hESCs. *Dev Biol* 357:492-504.
17. Zorn AM and JM Wells. (2009). Vertebrate endoderm development and organ formation. *Annu Rev Cell Dev Biol* 25:221-51.
18. Zaret KS. (2002). Regulatory phases of early liver development: paradigms of organogenesis. *Nat Rev Genet* 3:499-512.
19. Lemaigre F and KS Zaret. (2004). Liver development update: new embryo models, cell lineage control, and morphogenesis. *Curr Opin Genet Dev* 14:582-90.
20. Bendall SC, EF Simonds, P Qiu, AD Amir el, PO Krutzik, R Finck, RV Bruggner, R Melamed, A Trejo, OI Ornatsky, RS Balderas, SK Plevritis, K Sachs, D Pe'er, SD Tanner and GP Nolan. (2011). Single-cell mass cytometry of differential immune and drug responses across a human hematopoietic continuum. *Science* 332:687-96.
21. Bjornson ZB, GP Nolan and WJ Fantl. (2013). Single-cell mass cytometry for analysis of immune system functional states. *Curr Opin Immunol* 25:484-94.
22. Bendall SC and GP Nolan. (2012). From single cells to deep phenotypes in cancer. *Nat Biotechnol* 30:639-47.
23. Qiu P, EF Simonds, SC Bendall, KD Gibbs, Jr., RV Bruggner, MD Linderman, K Sachs, GP Nolan and SK Plevritis. (2011). Extracting a cellular hierarchy from high-dimensional cytometry data with SPADE. *Nat Biotechnol* 29:886-91.
24. Du P, WA Kibbe and SM Lin. (2008). lumi: a pipeline for processing Illumina microarray. *Bioinformatics* 24:1547-8.

25. Gadgil M, S Mehra, V Kapur and WS Hu. (2006). TimeView: for comparative gene expression analysis. *Appl Bioinformatics* 5:41-4.
26. Rossi JM, NR Dunn, BL Hogan and KS Zaret. (2001). Distinct mesodermal signals, including BMPs from the septum transversum mesenchyme, are required in combination for hepatogenesis from the endoderm. *Genes Dev* 15:1998-2009.
27. Radzisheuskaya A, B Chia Gle, RL dos Santos, TW Theunissen, LF Castro, J Nichols and JC Silva. (2013). A defined Oct4 level governs cell state transitions of pluripotency entry and differentiation into all embryonic lineages. *Nat Cell Biol* 15:579-90.
28. Yasunaga M, S Tada, S Torikai-Nishikawa, Y Nakano, M Okada, LM Jakt, S Nishikawa, T Chiba, T Era and S Nishikawa. (2005). Induction and monitoring of definitive and visceral endoderm differentiation of mouse ES cells. *Nat Biotechnol* 23:1542-50.
29. Nava S, M Westgren, M Jaksch, A Tibell, U Broome, BG Ericzon and S Sumitran-Holgersson. (2005). Characterization of cells in the developing human liver. *Differentiation* 73:249-60.
30. Carpenter AE, TR Jones, MR Lamprecht, C Clarke, IH Kang, O Friman, DA Guertin, JH Chang, RA Lindquist, J Moffat, P Golland and DM Sabatini. (2006). CellProfiler: image analysis software for identifying and quantifying cell phenotypes. *Genome Biol* 7:R100.
31. Chen J and K Raymond. (2006). Roles of rifampicin in drug-drug interactions: underlying molecular mechanisms involving the nuclear pregnane X receptor. *Ann Clin Microbiol Antimicrob* 5:3.

32. Yao Y, R Liu, MS Shin, M Trentalange, H Allore, A Nassar, I Kang, JS Pober and RR Montgomery. (2014). CyTOF supports efficient detection of immune cell subsets from small samples. *J Immunol Methods* 415:1-5.
33. Sen N, G Mukherjee, A Sen, SC Bendall, P Sung, GP Nolan and AM Arvin. (2014). Single-cell mass cytometry analysis of human tonsil T cell remodeling by varicella zoster virus. *Cell Rep* 8:633-45.
34. Chang Q, OI Ornatsky, CJ Koch, N Chaudary, DT Marie-Egyptienne, RP Hill, SD Tanner and DW Hedley. (2015). Single-cell measurement of the uptake, intratumoral distribution and cell cycle effects of cisplatin using mass cytometry. *Int J Cancer* 136:1202-9.
35. Ornatsky O, D Bandura, V Baranov, M Nitz, MA Winnik and S Tanner. (2010). Highly multiparametric analysis by mass cytometry. *J Immunol Methods* 361:1-20.
36. Giesen C, HA Wang, D Schapiro, N Zivanovic, A Jacobs, B Hattendorf, PJ Schuffler, D Grolimund, JM Buhmann, S Brandt, Z Varga, PJ Wild, D Gunther and B Bodenmiller. (2014). Highly multiplexed imaging of tumor tissues with subcellular resolution by mass cytometry. *Nat Methods* 11:417-22.
37. Lujan E, ER Zunder, YH Ng, IN Goronzy, GP Nolan and M Wernig. (2015). Early reprogramming regulators identified by prospective isolation and mass cytometry. *Nature* 521:352-6.

Figure Legends

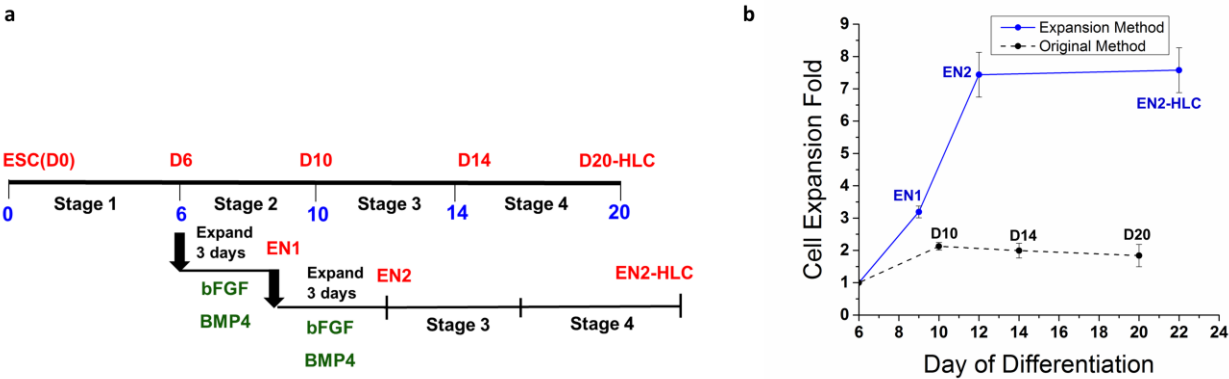


Figure 1. Protocol for expansion of hepatic endodermal cells.

(a) Four stage directed hepatic differentiation protocol and the modified protocol with cell expansion in Stage 2. For expansion, cells at the endodermal stage (D6) were subcultured for 3 days (EN1) and subcultured again for another 3 day (EN2) in Stage 2 medium. The expanded hepatic endodermal cells (EN2) were then continued to be cultured in Stage 3 and Stage 4 medium to become EN2-HLC. The cells derived with the conventional protocol are denoted as D20-HLC.

(b) Increasing cell number during the course of cell expansion and regular differentiation. All error bars are represented as SD. (n=4)

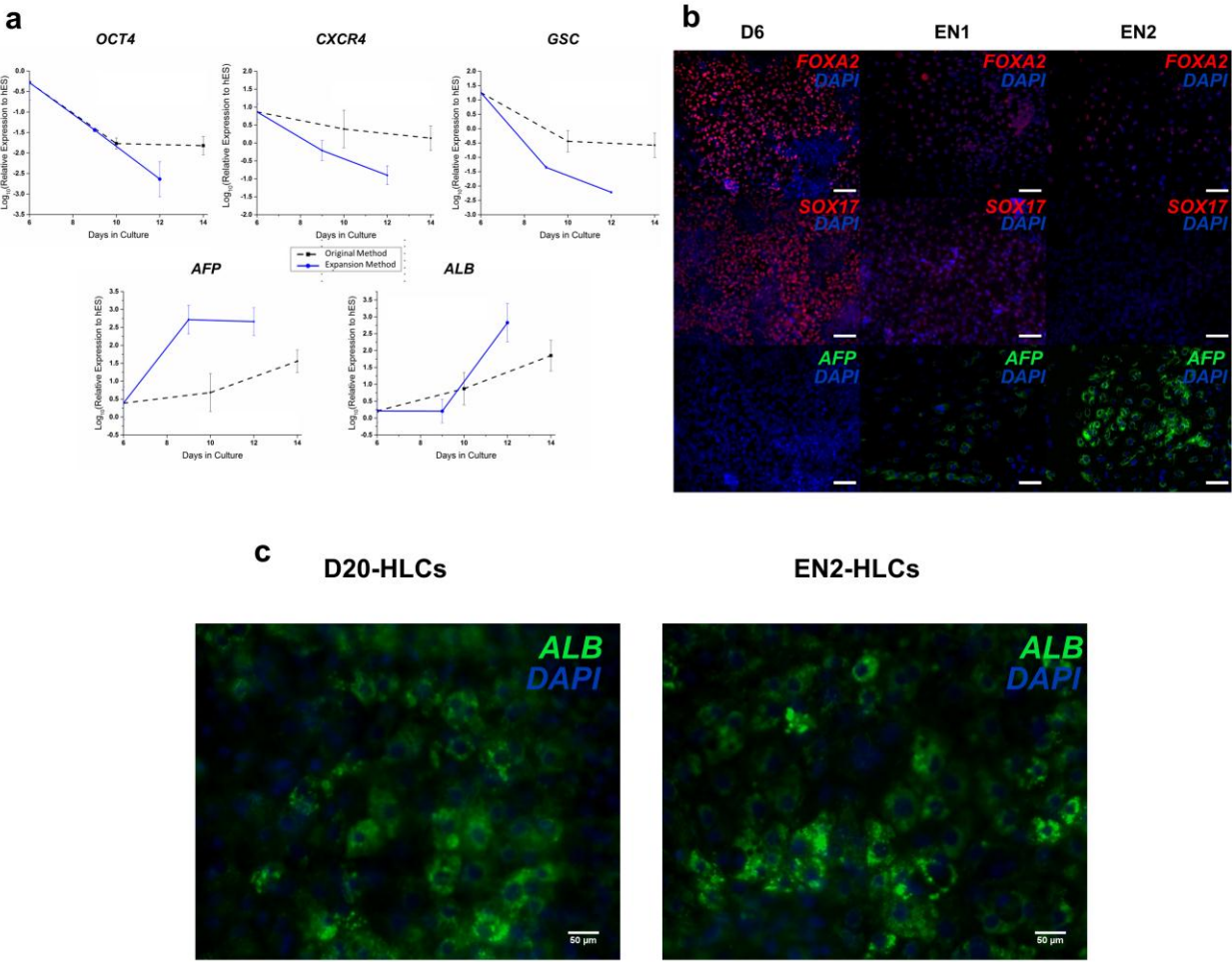


Figure 2. Phenotype of endodermal cells undergoing expansion.

(a) Transcript level of marker genes in endodermal cells and their subsequent expansion stage. During D6, endodermal markers were prominent (*CXCR4*, *GSC*) and pluripotent markers were still present (*OCT4*). During the original method of

differentiation (D10 and D14) and the corresponding expansion stages (EN1 and E2), expression of pluripotent and endoderm markers decreased while hepatic markers (*AFP* and *ALB*) began to increase. All error bars are represented as SD. (n=4)

(b) Immunostaining of endodermal cells undergoing simultaneous differentiation and expansion. Endodermal markers (FOXA2 and SOX17) were expressed in D6 cells but decreased in EN1 and EN2 cells. AFP expression increased in EN1 and EN2 cells.

Scale bar = 150 μ m.

(c) Immunostaining of D20-HLCs and EN2-HLCs showing albumin expression.

Scale bar = 50 μ m.

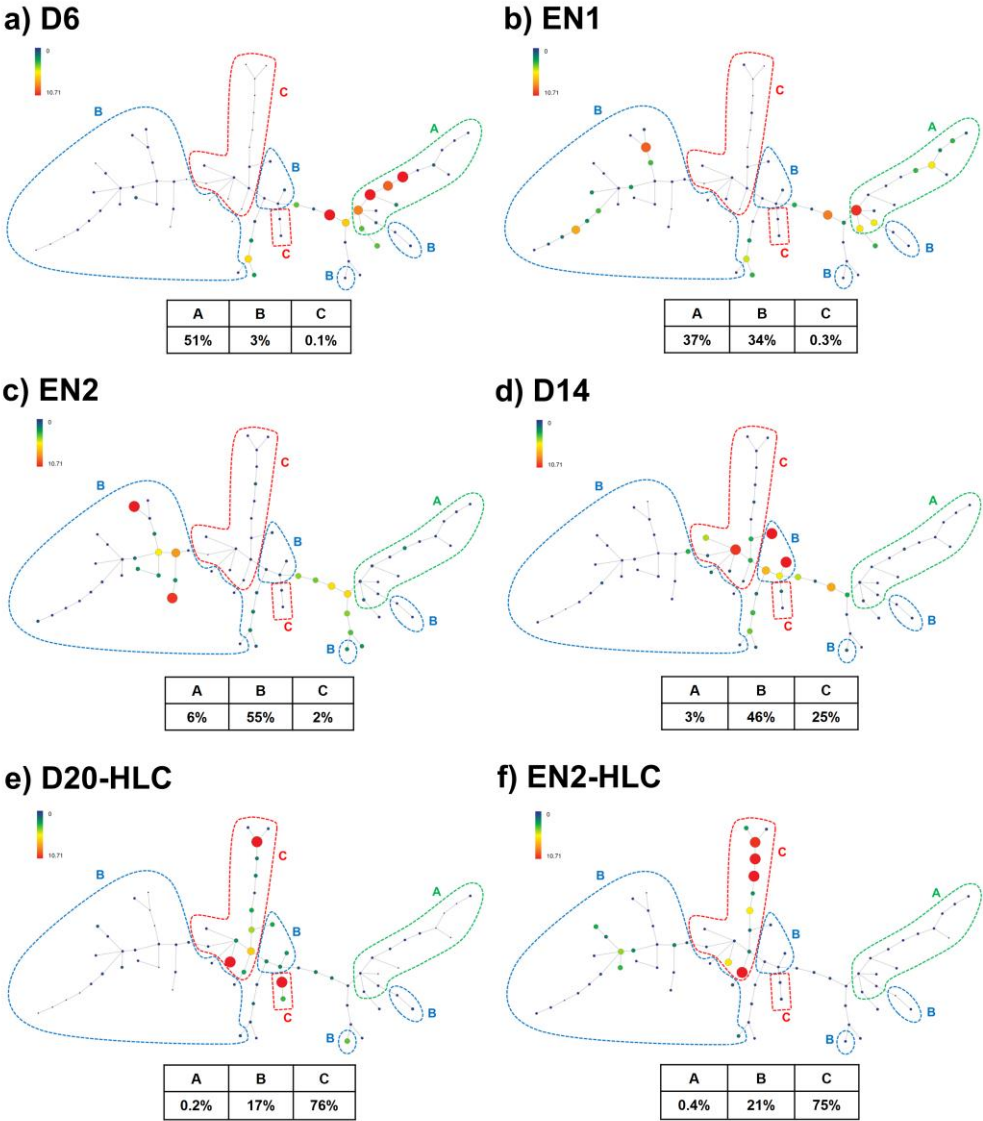


Figure 3. SPADE analysis of mass cytometry data of cells differentiating toward HLCs.

The mass cytometry data of cells at different differentiation stages were clustered into 75 nodes by SPADE analysis. SPADE results for D6, EN1, EN2, D14, D20-HLC, and EN2-HLC are shown. The color and the size of a node represent percentage of the

populations for the node in each sample. Subpopulations enclosed in A, B, and C are classified as endodermal cells, hepatic endoderm/hepatoblasts, and hepatoblasts/hepatocytes, respectively. The methods for the classification of these subpopulations are described in detail in Figure S6. The percentage of endodermal cells, hepatic endoderm/hepatoblasts, and hepatoblasts/hepatocytes for each population is shown.

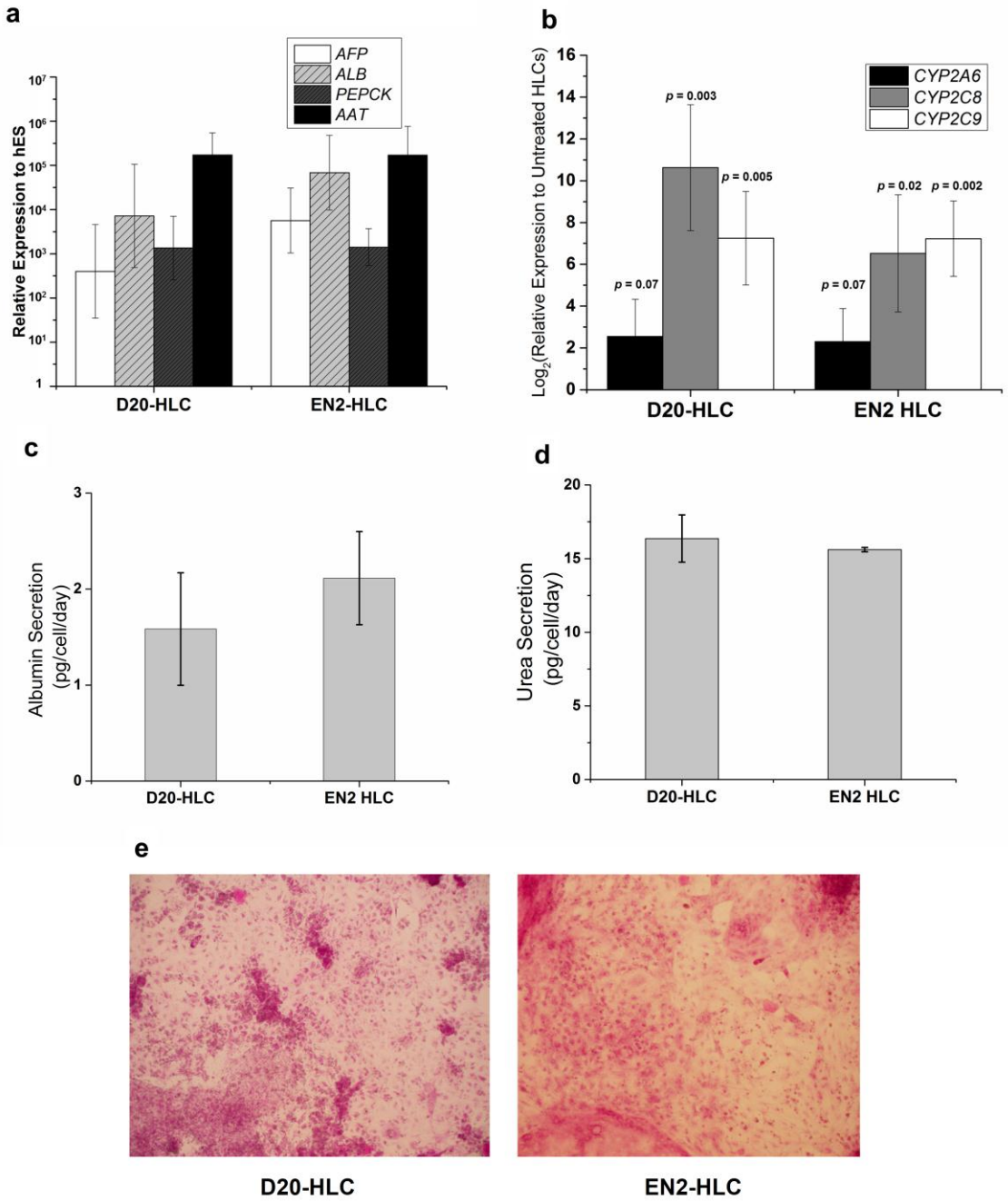


Figure 4. Transcript level of hepatic markers in D20-HLCs and EN2-HLCs.

(a) D20-HLCs and EN2-HLC both expressed transcripts of hepatocyte markers *AFP*, *ALB*, *AAT* and *PEPCK*. (b) Transcript level change of *CYP2A6*, *CYP2C8* and *CYP2C9*

in D20-HLCs and EN2-HLCs after induction with rifampicin. p-values of Student's t-test are shown. (c-d) Activities of albumin secretion and urea synthesis of D20-HLCs and EN2-HLCs. The standard deviations of three biological replica are shown. (e) Glycogen staining of D20-HLCs and EN2-HLCs.

All error bars are represented as SD. (n=3)

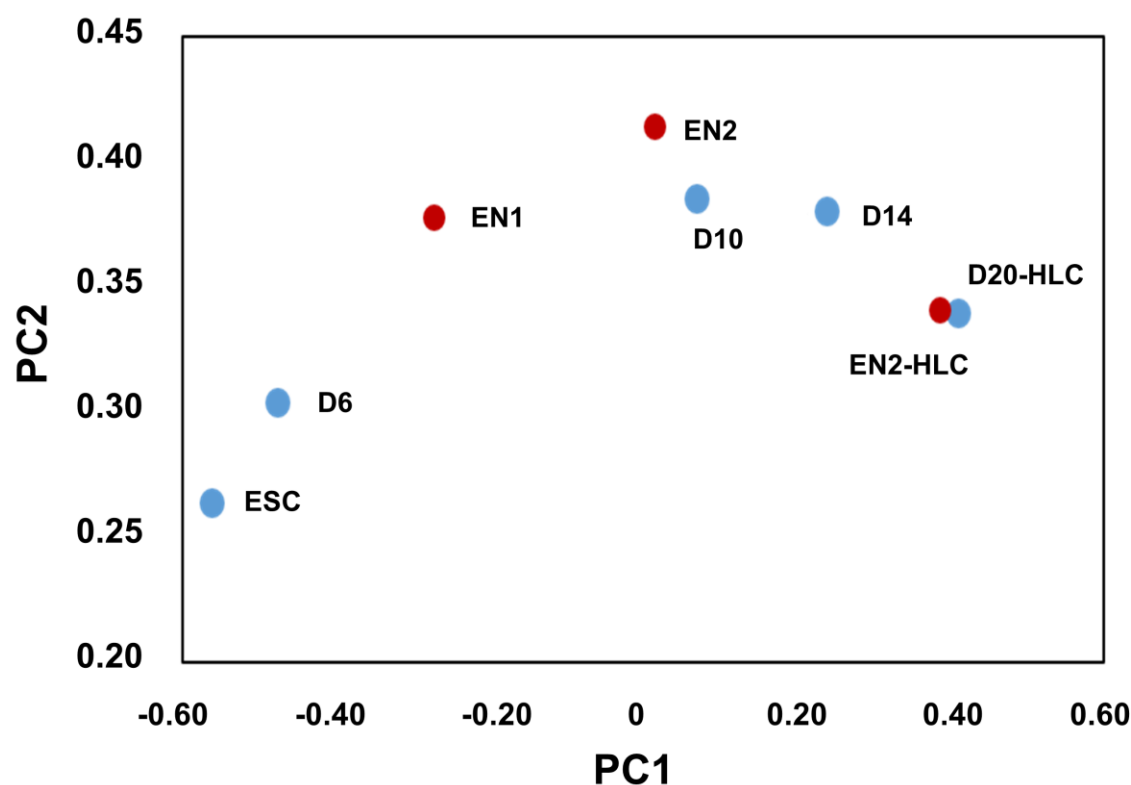


Figure 5. Transcriptome analysis of differentiating and expanding cells.

Cell samples at different differentiation stages from the conventional protocol (blue) and expanding protocol (red) align along the same PC space (PC1 vs. PC2). EN1 and EN2 samples are in between D6 and D10 (the beginning and end of Stage 2 differentiation of the conventional protocol).

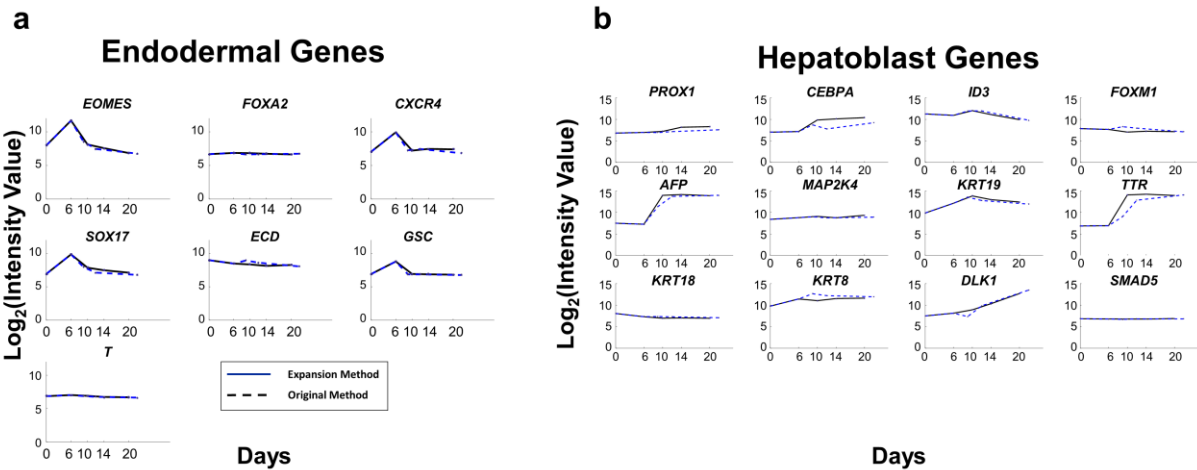


Figure 6. Transcript levels of stage-specific markers.

Dynamics of key (a) endoderm markers and (b) hepatoblast markers are similar in cells differentiated with the two different protocols (dashed = original method, solid = expansion method).

Supplementary Figures

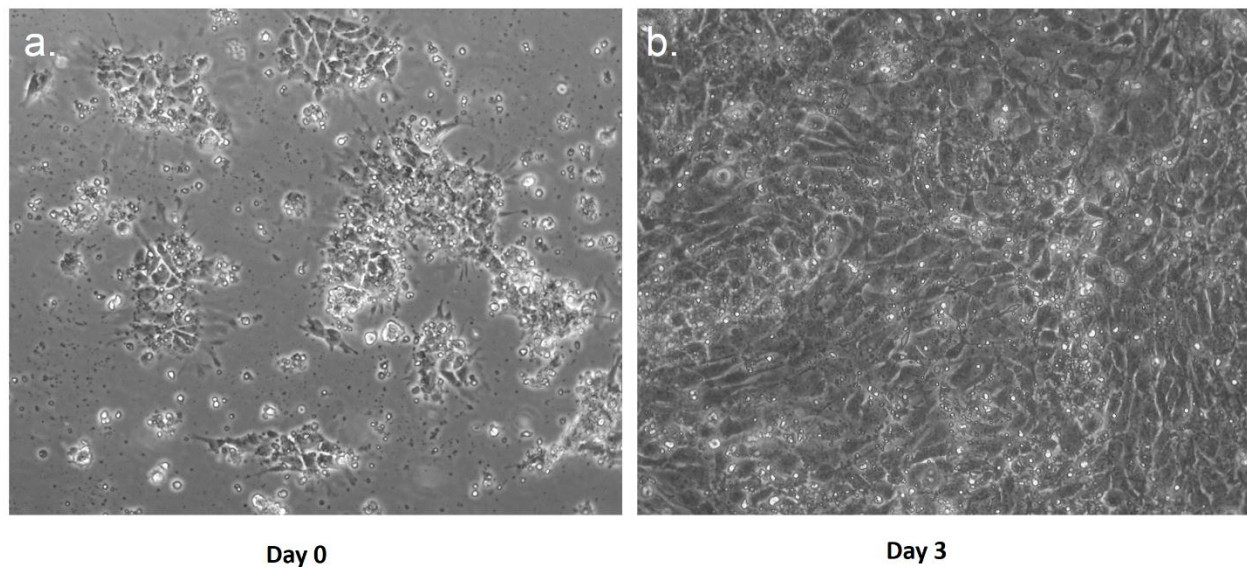


Figure S1. Morphology of endodermal cells expanding

a) Immediately after plating and b) after three days in Stage 2 conditions

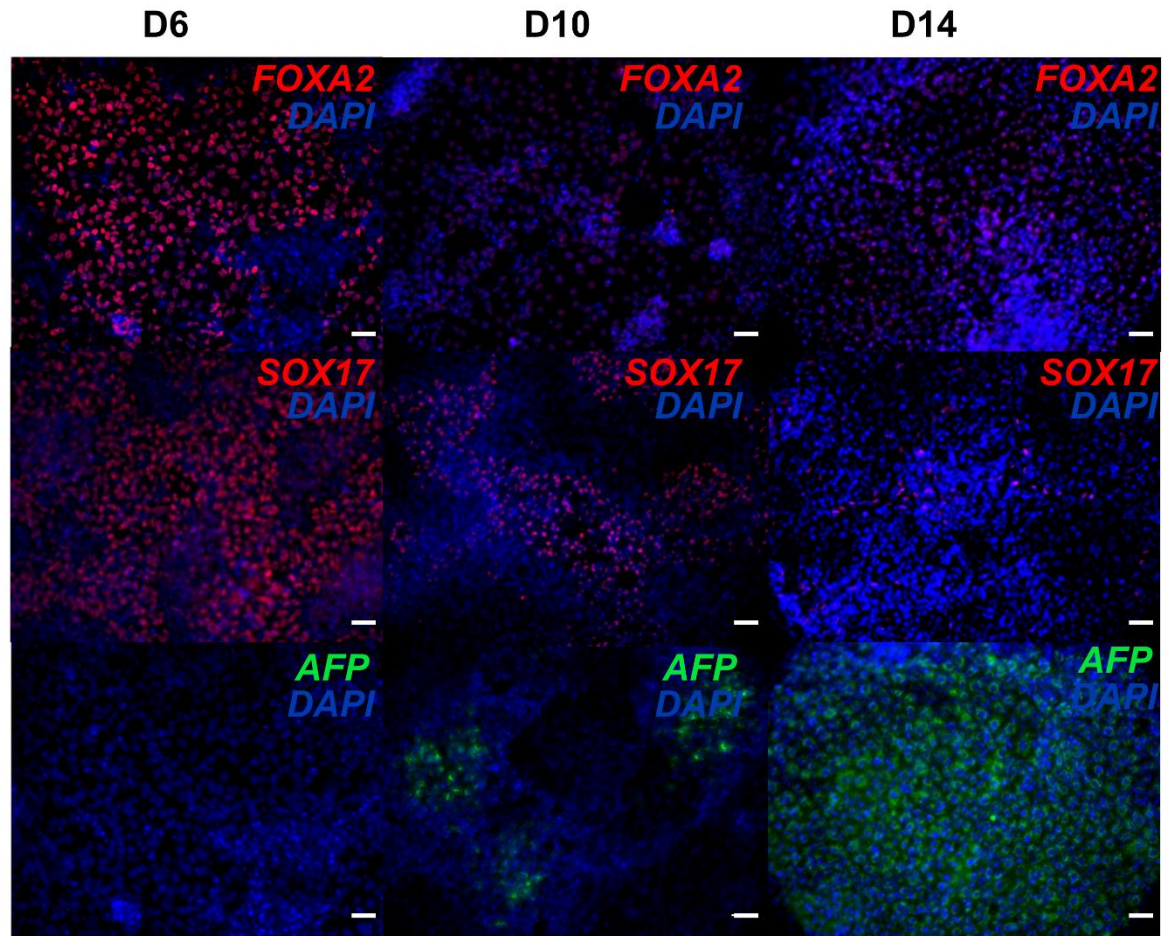


Figure S2. Immunohistochemistry of endodermal cells during differentiation. Immunostaining of endodermal cells undergoing the conventional method of differentiation. Endodermal markers (FOXA2 and SOX17) were expressed in D6 cells and continued to be increased through day 14 but SOX17 expression is drastically decreased by day 14. AFP expression increases gradually from day 6 to until day 14 where a majority of the cells are positive for AFP. Scale bar = 150 μ m.

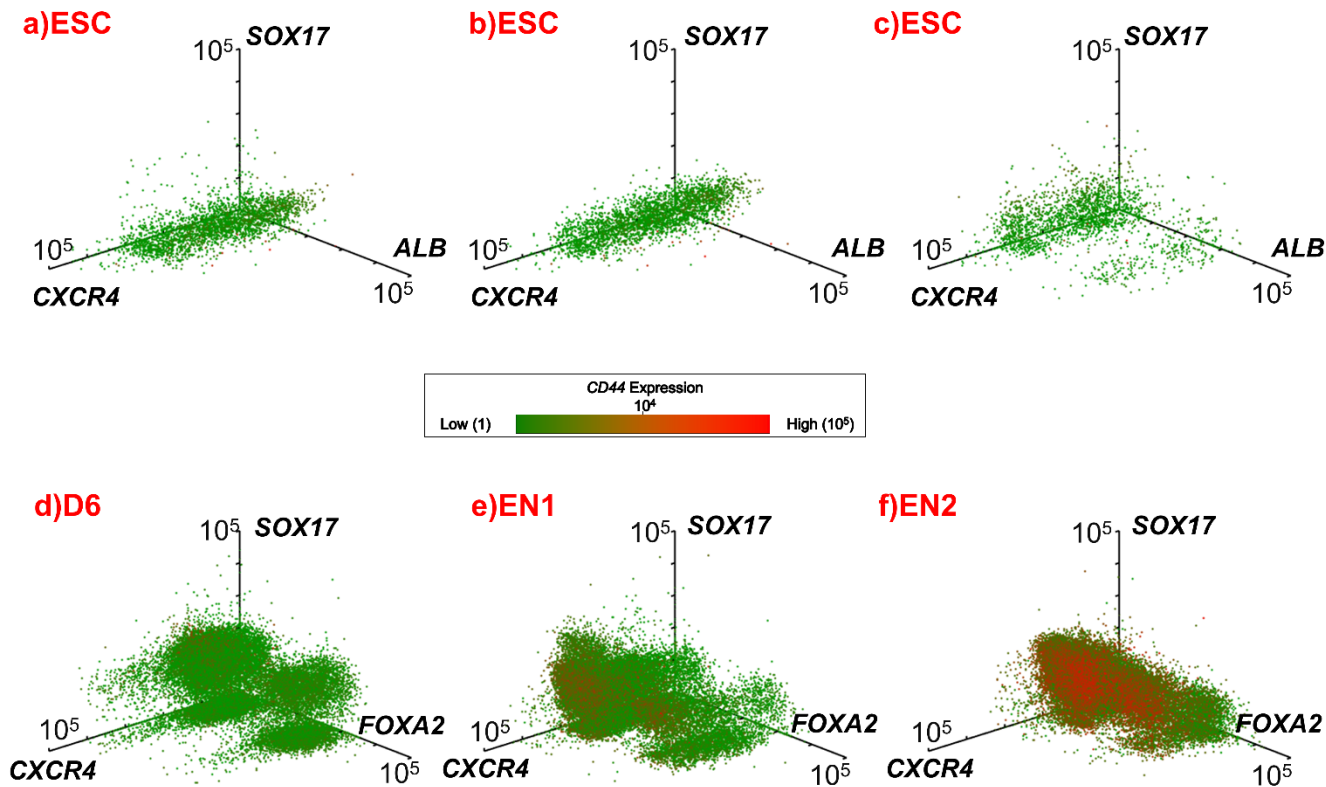


Figure S3. Mass cytometry analysis

Mass cytometry data is represented as a three-dimensional scatter plot with color representing the fourth dimension. The axes show the expression of different markers FOXA2, SOX17, CXCR4, *DLK1*, and *ALB* and the color gradient of each dot show the expression of CD44. The negative control for the markers used was hESCs which shows low expression for hepatic markers (*DLK1* and *ALB*). As the cells undergo endodermal expansion, the endodermal genes decrease and CD44 expression increases. The presence of CD44 has been shown to play an important role in HGF-induced signaling by promoting autophosphorylation of the HGF receptor, c-MET [29].

Thus, CD44 is typically used as a marker for a subpopulation of hepatic progenitor cells that have high growth potential in culture [30]. The protein levels of SOX17 and CXCR4, very low in ESC (Figure S4a-c), began to be co-expressed in a distinct population (Figure S4d). During the course of the endodermal expansion, a very large fraction of cells co-expressing SOX17 and CXCR4 started to express CD44 (Figure S4d-f).

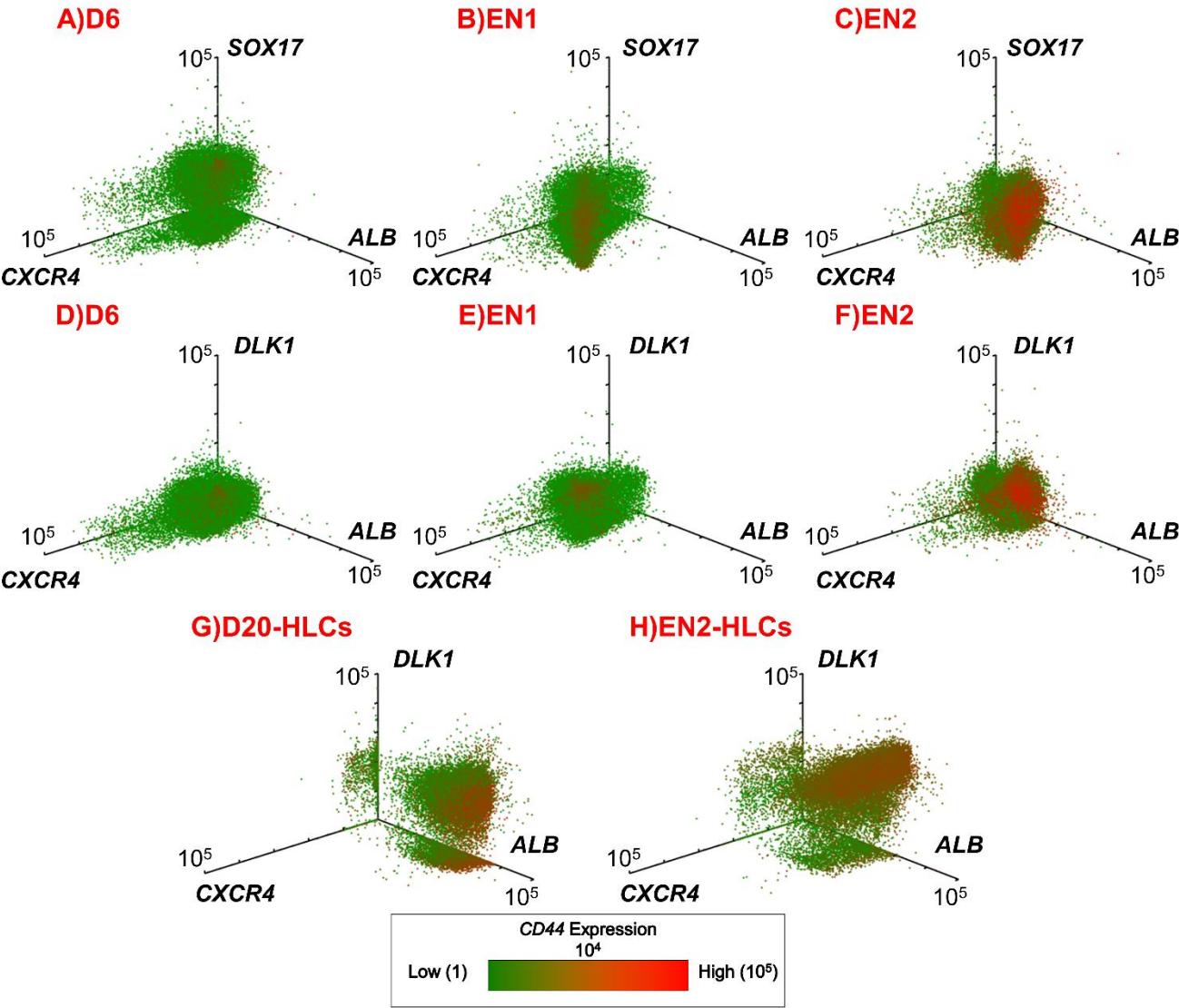


Figure S4. Mass cytometry analysis

Mass cytometry data is represented as a three-dimensional scatter plot with color representing the fourth dimension. The axes show the expression of different hepatic and endoderm markers ALB, SOX17, CXCR4, or DLK1 and the colored dots show the expression of CD44. As the cells undergo endodermal expansion, the endodermal

genes decrease and CD44 expression increases. Evaluation of the expanding D6 population illustrated that the bulk of the cell population expressing both ALB and CD44 also simultaneously lose expression of the endodermal markers, SOX17 and CXCR4, in line with results from qRT-PCR and immunostaining (Figure 2). DLK1 has frequently been used as a marker for early hepatocyte committed progenitor cells that can be isolated from the embryonic liver *in vivo* [31, 32]. Using DLK1 as a marker for hepatocyte-committed cells, a large fraction of the expanding EN1 and EN2 population began to gain DLK1 expression giving credence to the assignment of early hepatic subpopulation. The expression of CD44 and ALB were gradually increasing along with DLK1, showing co-expression of all three hepatoblast markers in the majority of DLK1 positive cells. The co-expression of hepatoblast markers observed in the D20-HLCs and EN2-HLCs populations further illustrates that the majority of the cells are capable of differentiating towards the hepatocyte lineage regardless of whether or not they were subjected to endodermal expansion steps (Figure S5g and S5h). Notably both D20-HLCs and EN2-HLCs showed low expression levels of CXCR4.

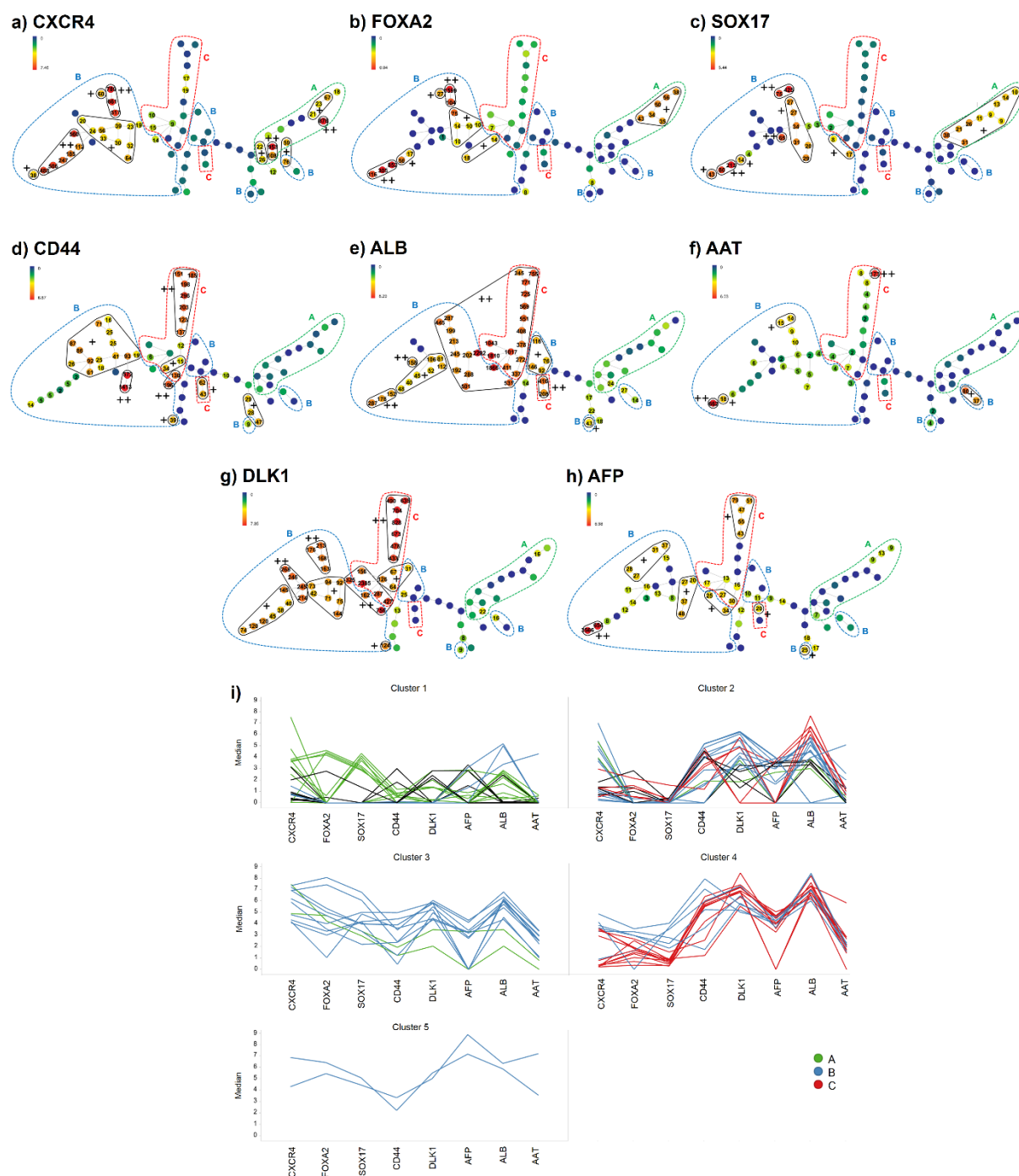


Figure S5. SPADE analysis of Mass cytometry data.

(a-h) The expression level of each of 8 markers is shown in a separate tree diagram. The color represents arcsinh transformed intensity of each marker. Median of the intensity for a node is shown. The expression level of each marker is ranked as high (++), moderate (+), and low (-). The threshold for ++ and + is 100 and 20 for CXCR4, 100 and 10 for FOXA2, 60 and 8 for SOX17, 100 and 15 for CD44, 150 and 40 for ALB, 100 and 14 for AAT, 150 and 30 for DLK1, and 100 and 20 for AFP, respectively. Unannotated parts of the SPADE tree for each marker were considered as the cells with low (-) expression of the marker. The nodes enclosed in A, B, and C are classified as endodermal cells, hepatic endoderm/hepatoblasts, and hepatoblasts/hepatocytes, respectively. The following expression patterns were used to classify the subpopulations: (A) $(CXCR4^{++/+} \cup FOXA2^{++/+} \cup SOX17^{++/+}) \cap DLK1^{-} \cap AFP^{-} \cap ALB1^{-} \cap AAT^{-}$ (“++/+” denotes ranging from ++ to +, and “ \cup ” and “ \cap ” represent union and intersection, respectively). (B) encompasses three subclasses: (i) $(CXCR4^{++/+} \cup FOXA2^{++/+} \cup SOX17^{++/+}) \cap (DLK1^{++/+} \cup AFP^{++/+} \cup ALB^{++/+} \cup AAT^{++/+})$, (ii) $CXCR4^{++/+} \cap FOXA2^{++/+} \cap SOX17^{++/+} \cap (DLK1^{++/+} \cup AFP^{++/+}) \cap ALB^{+/-} \cap AAT^{+/-}$, or (iii) $CXCR4^{++/+} \cap FOXA2^{++/+} \cap SOX17^{++/+} \cap DLK1^{++/+} \cap AFP^{++/+} \cap (ALB^{+} \cup AAT^{+})$. (C) $CXCR4^{-} \cap FOXA2^{-} \cap SOX17^{-} \cap DLK1^{++/+} \cap AFP^{++/+} \cap ALB^{++} \cup AAT^{++}$. i) K-means clustering was performed to the 75 nodes from the SPADE analysis based on the median intensity of the 8 markers (green lines: nodes in subpopulation A (endodermal cells), blue lines: nodes in subpopulation B (hepatic endoderm/hepatoblasts), red lines: nodes in subpopulation C (hepatoblasts/hepatocytes), and black lines: nodes not classified as any subpopulation). The distance was measured with Euclidean distance. 10 of the 14 nodes in the A subpopulation were in Cluster 1. 11 of the 16 nodes in the C subpopulation were in Cluster 4, revealing that majority of the nodes in A and C were separately clustered. The majority of the B nodes were intersperse into Clusters 2 and 3, with 12 and 10 of the B nodes in Clusters 2 and 3, respectively.

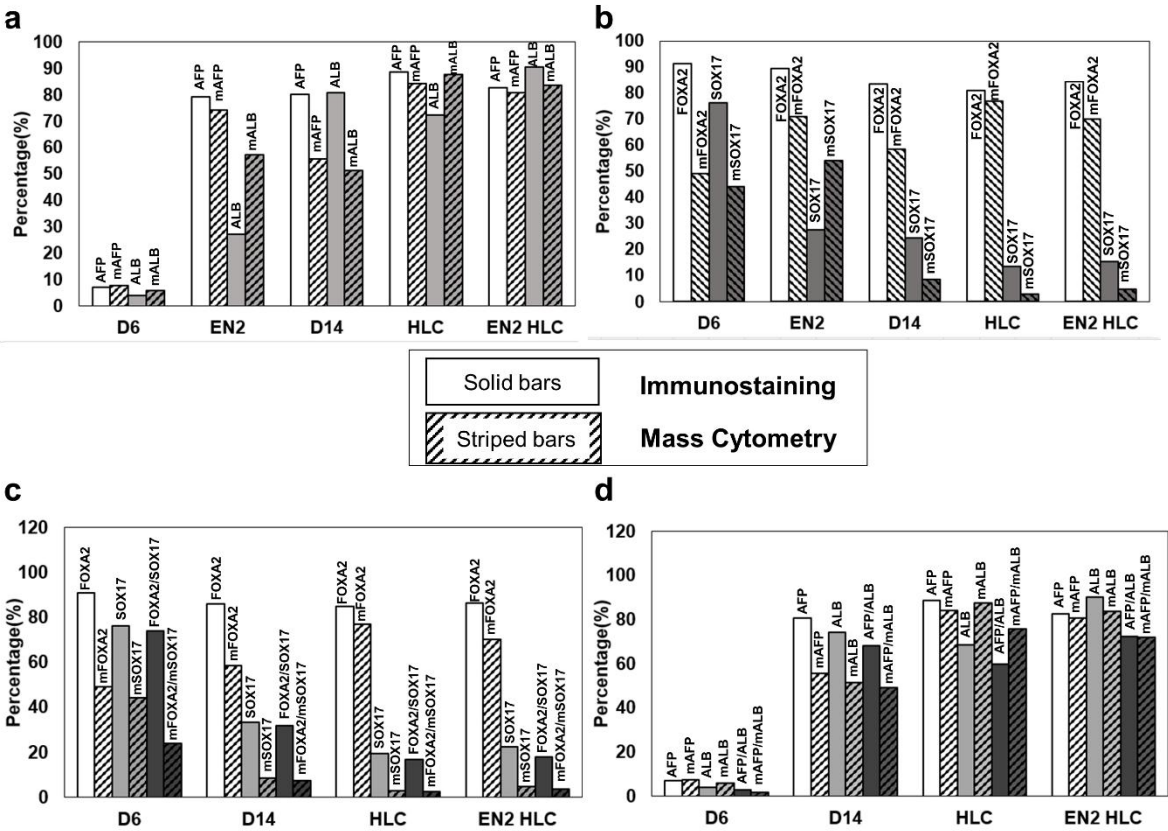


Figure S6. Mass cytometry and immunostaining of hepatic and endodermal markers. a) Immunostaining for AFP (white) and ALB (grey) was carried out at different stages of the differentiation along with the percentage of cells positive for AFP (white with lines) and ALB (grey with lines) found during mass cytometry. b) Immunostaining for FOXA2 (white) and SOX17 (grey) was carried out at different stages of the differentiation along with the percentage of cells positive for FOXA2 (white with lines) and SOX17 (grey with lines) found during mass cytometry. c) Co-staining was carried out for FOXA2 (white) and SOX17 (grey) where the percentages of double positive (dark grey) cells were quantified and also compared to mass cytometry percentages (stripe bars). d) Co-staining was carried out for AFP (white) and ALB (grey) where the percentages of double positive (dark grey) cells were quantified and also compared to mass cytometry percentages (stripe bars).

ESC Specific Genes

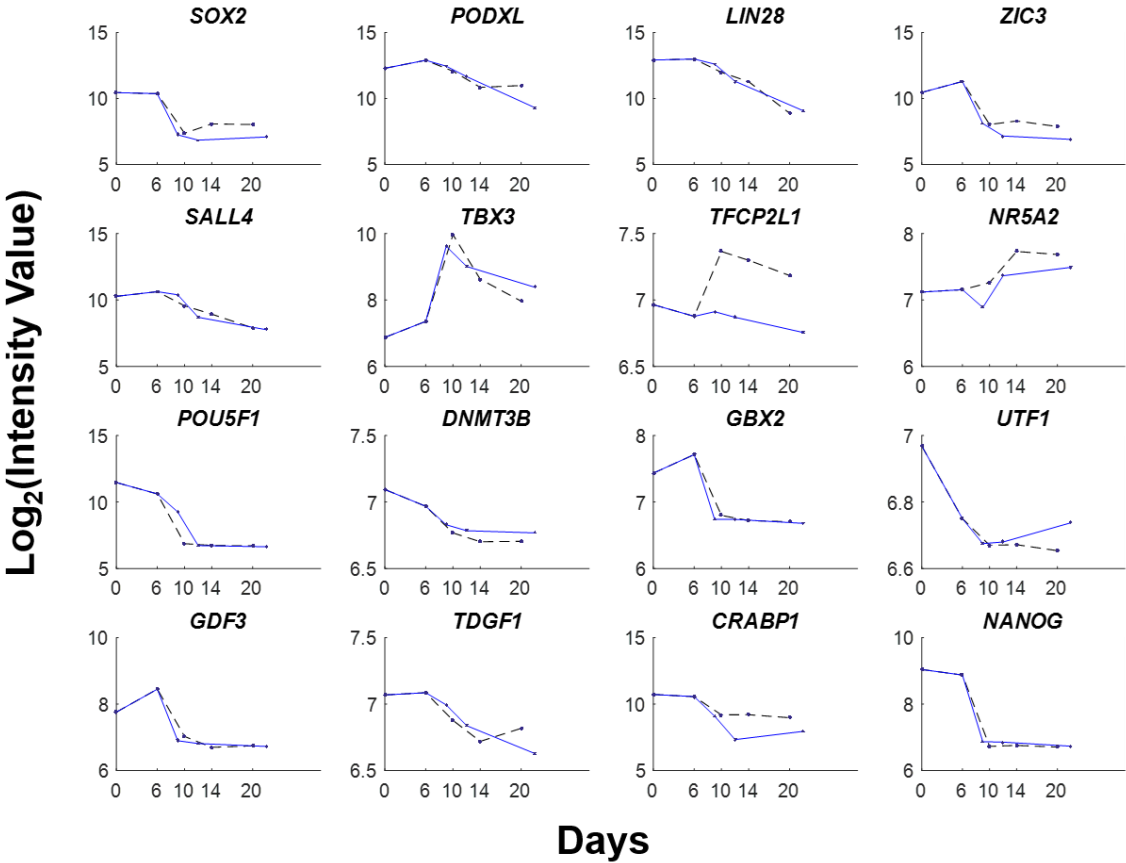
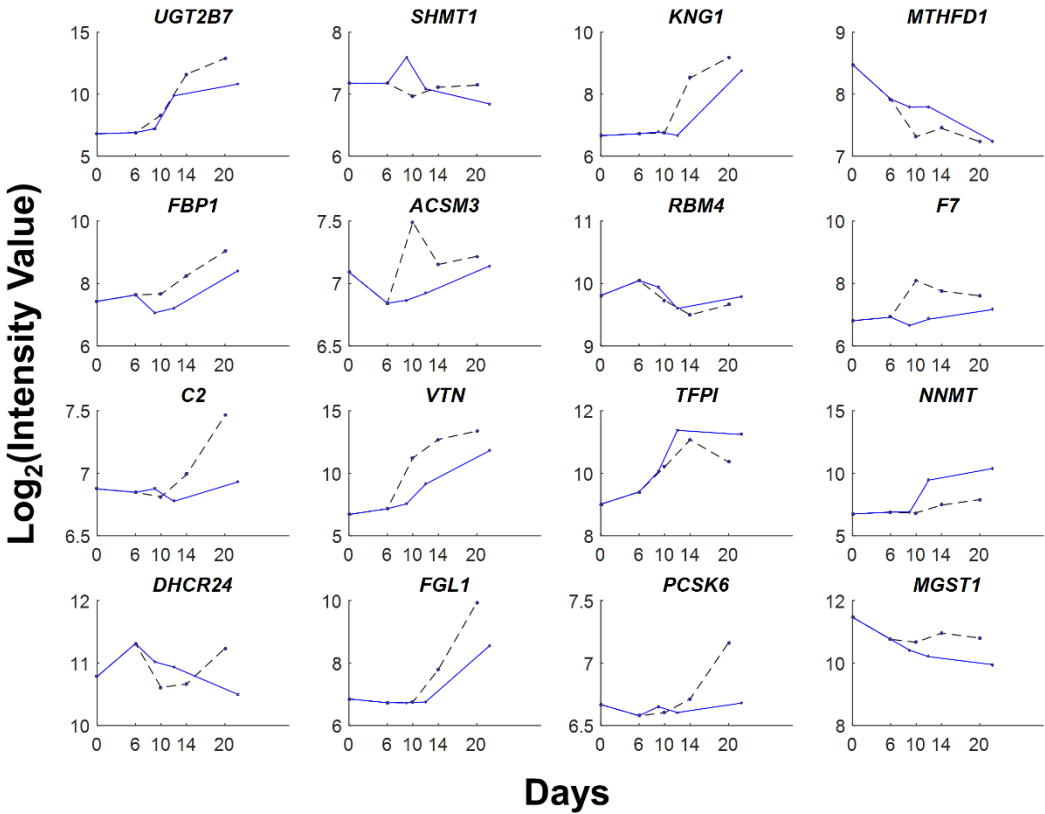


Figure S7. Transcript dynamics of embryonic stem cell specific genes during directed differentiation with the original protocol or with simultaneous expansion.

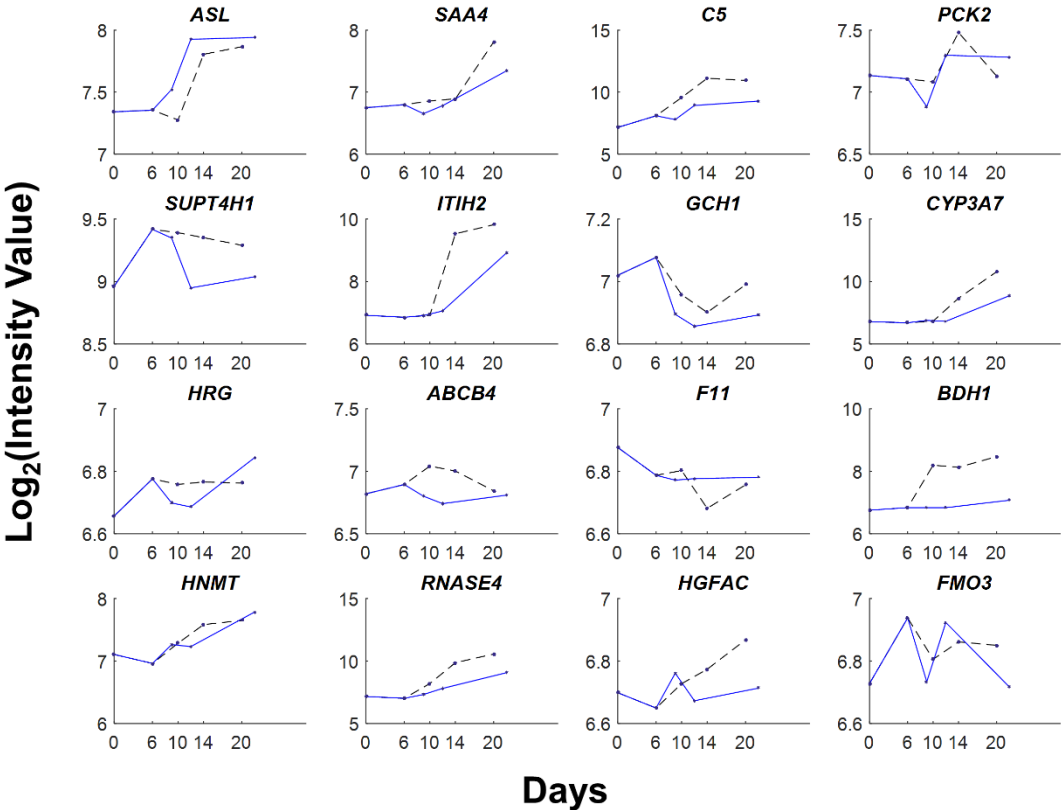
a

Liver Specific Genes



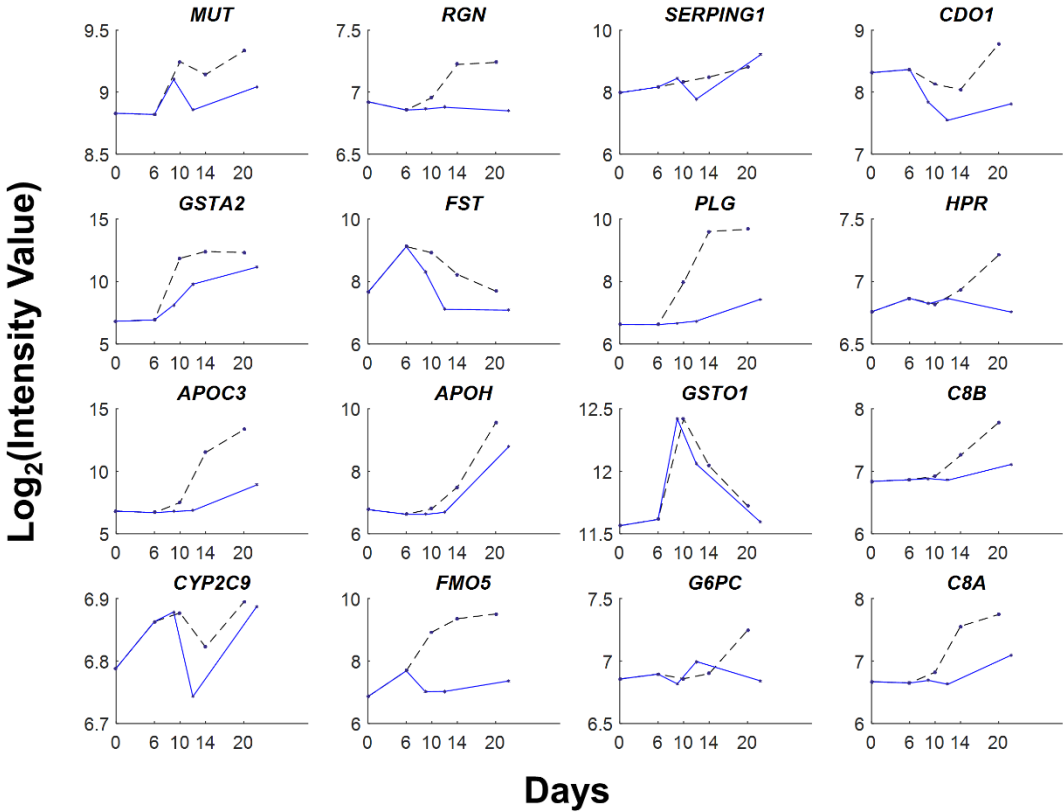
b

Liver Specific Genes



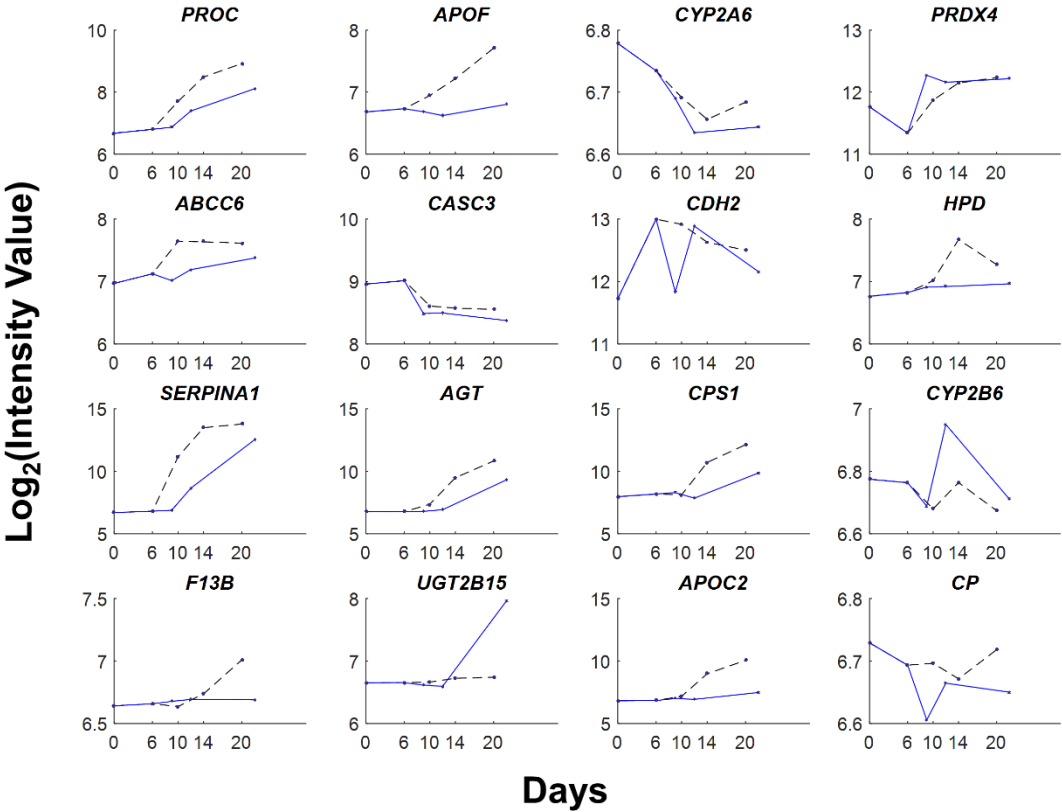
C

Liver Specific Genes



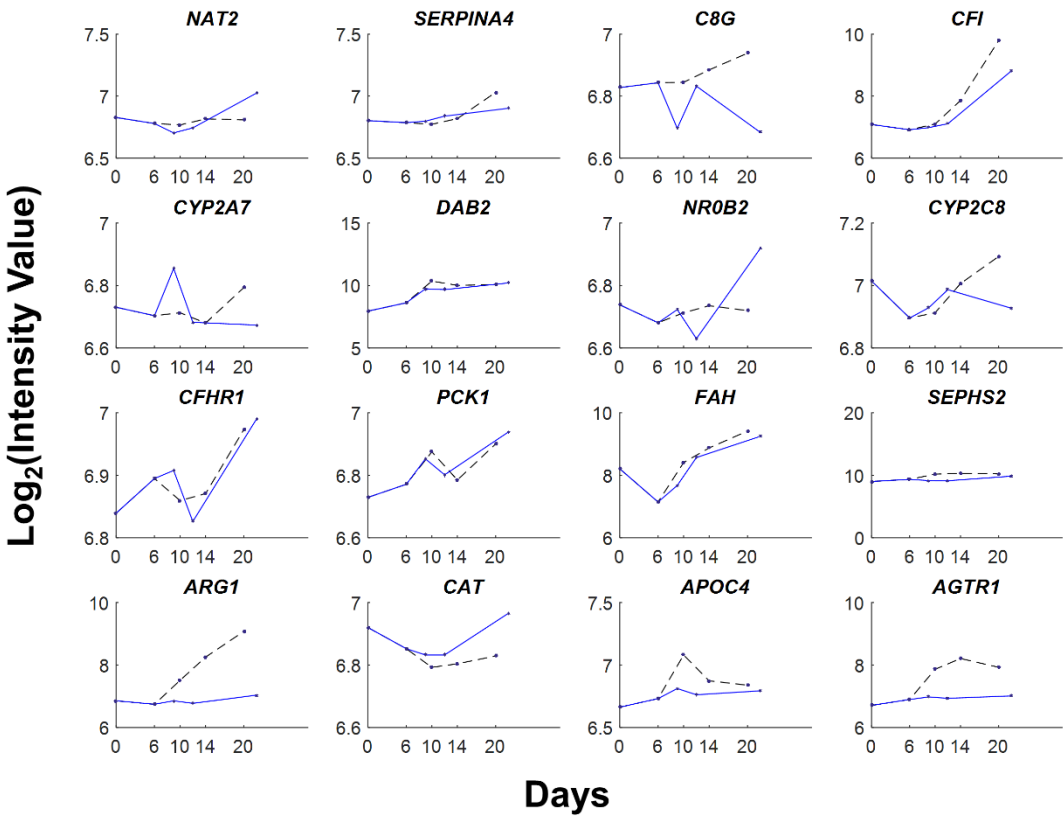
d

Liver Specific Genes



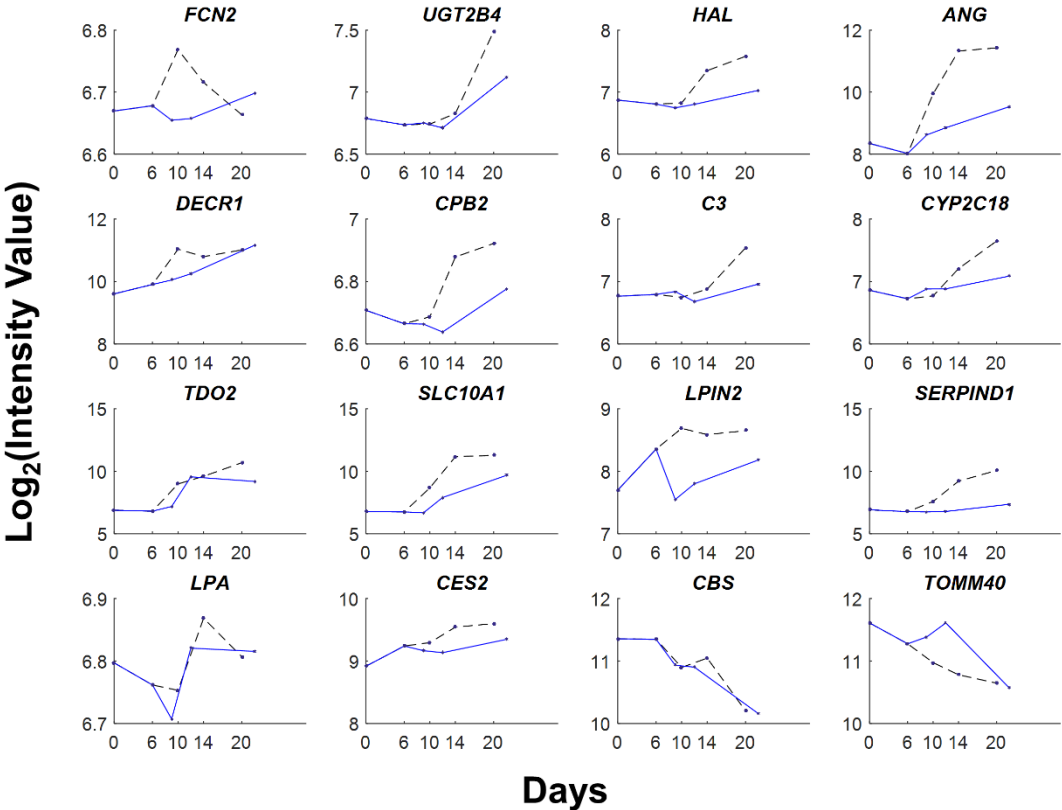
e

Liver Specific Genes



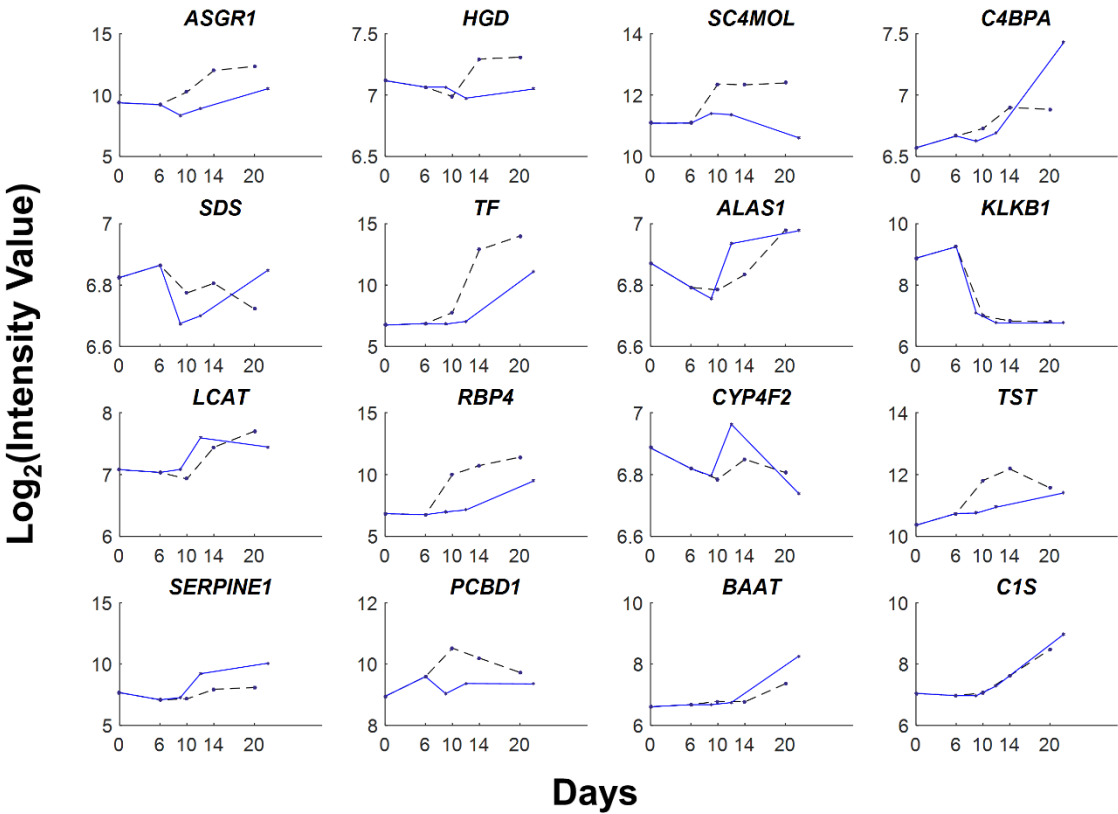
f

Liver Specific Genes



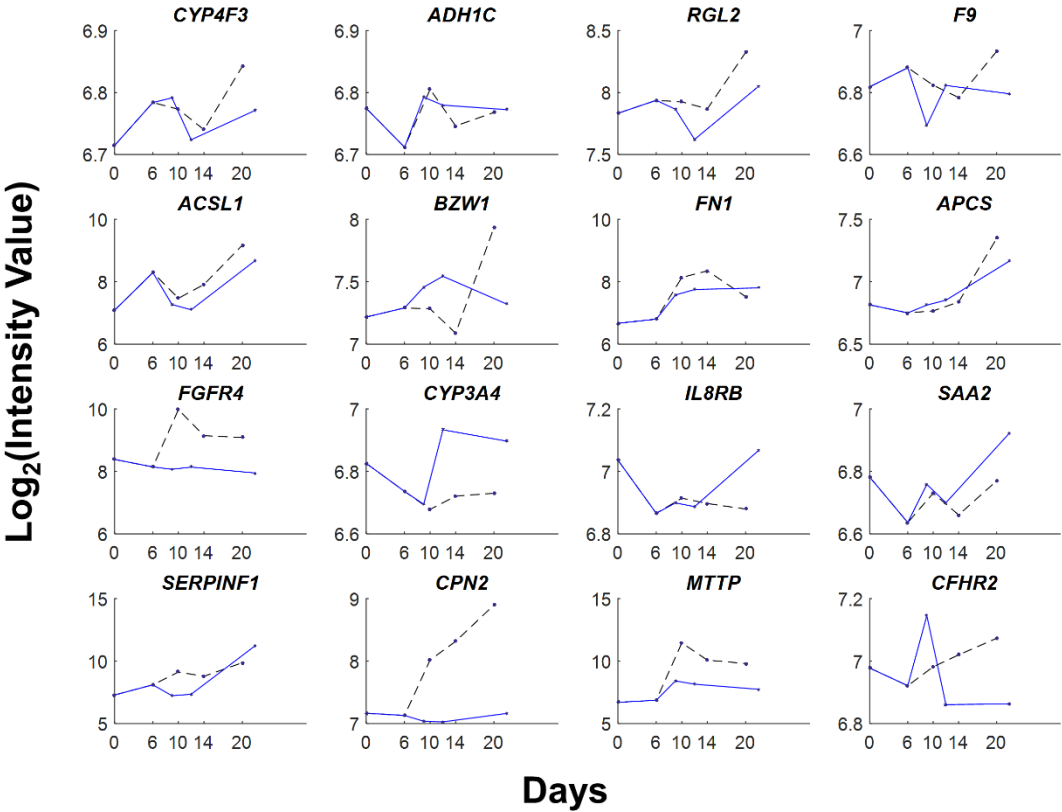
g

Liver Specific Genes

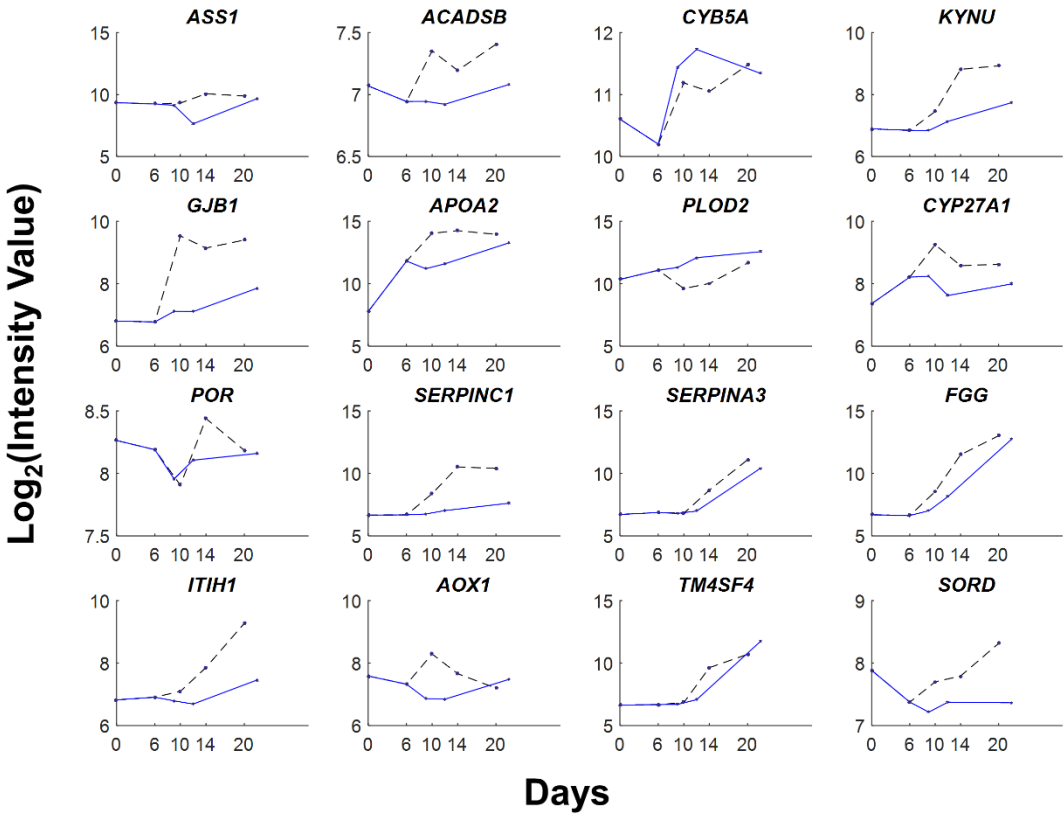


h

Liver Specific Genes

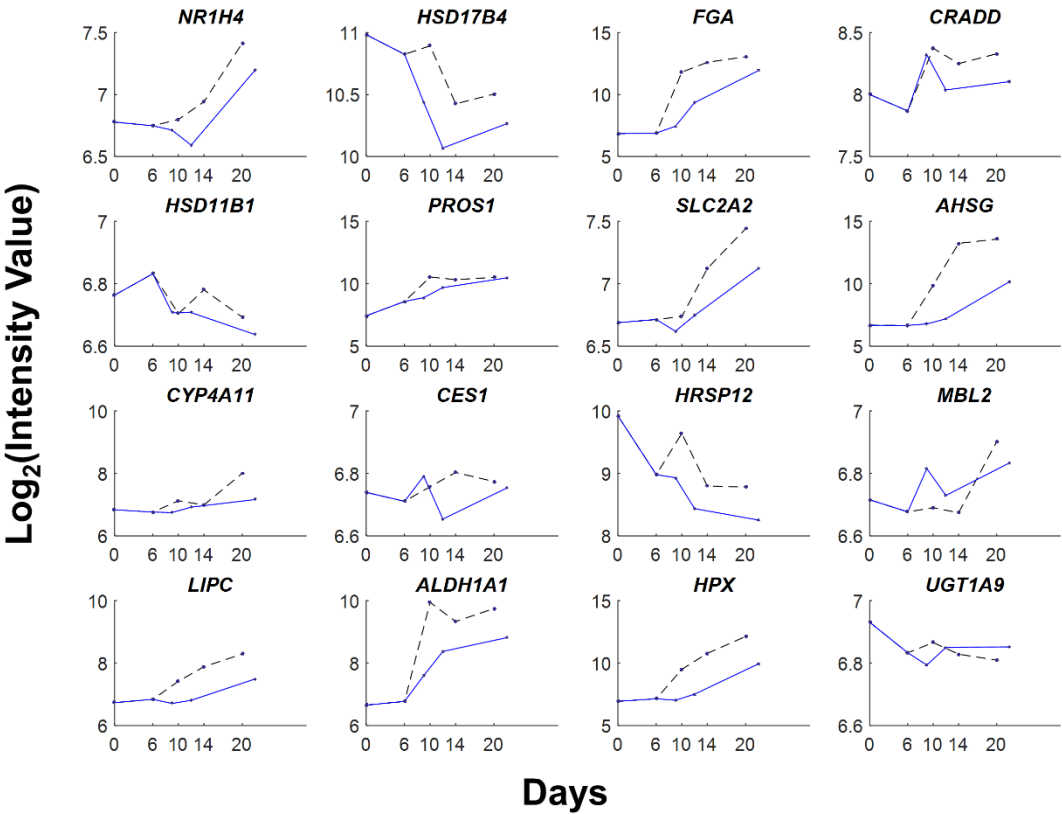


Liver Specific Genes



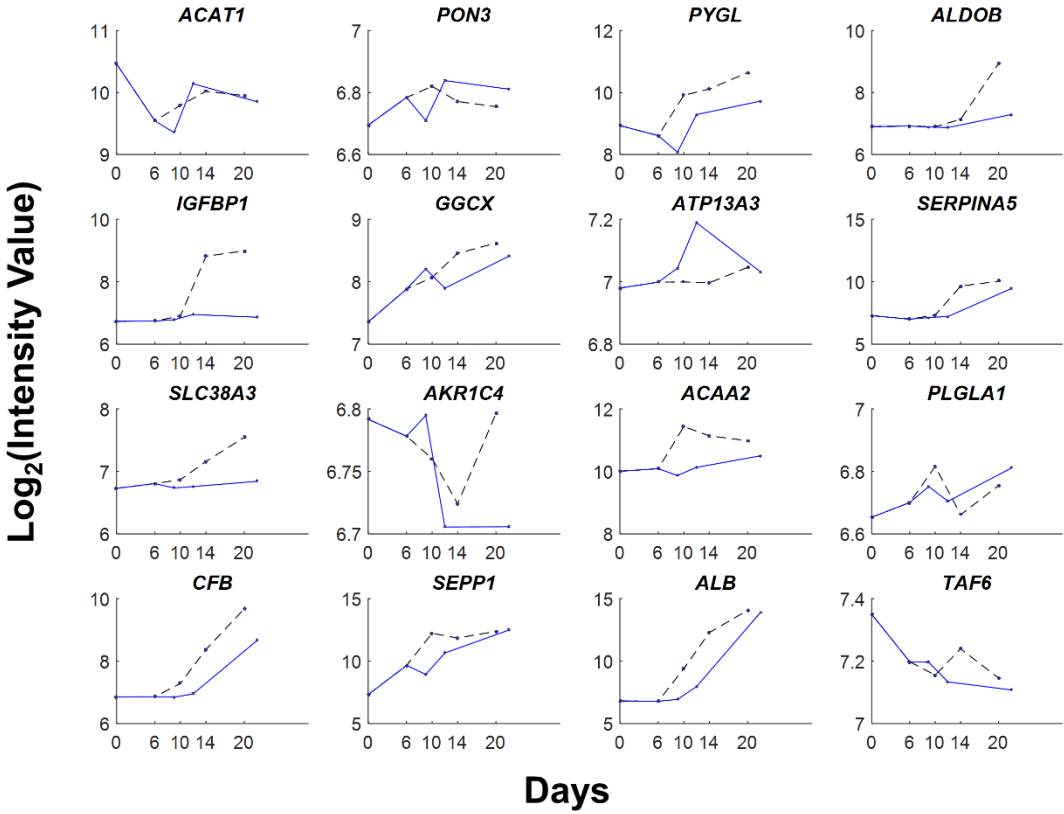
j

Liver Specific Genes

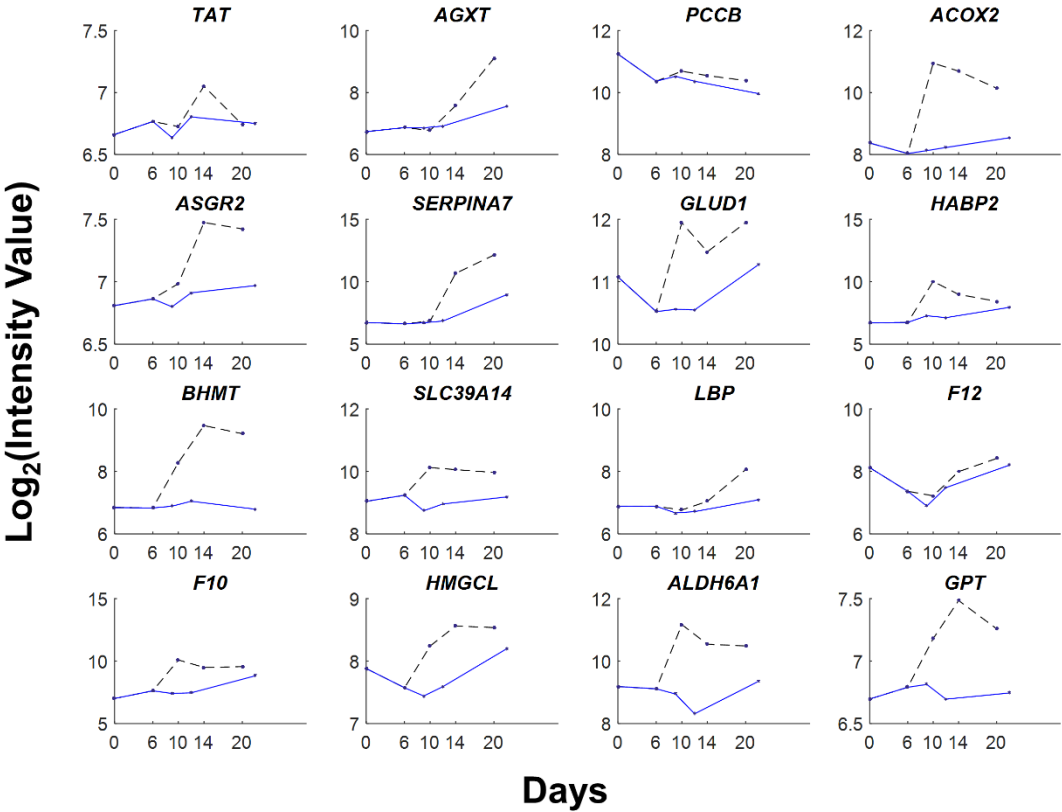


k

Liver Specific Genes

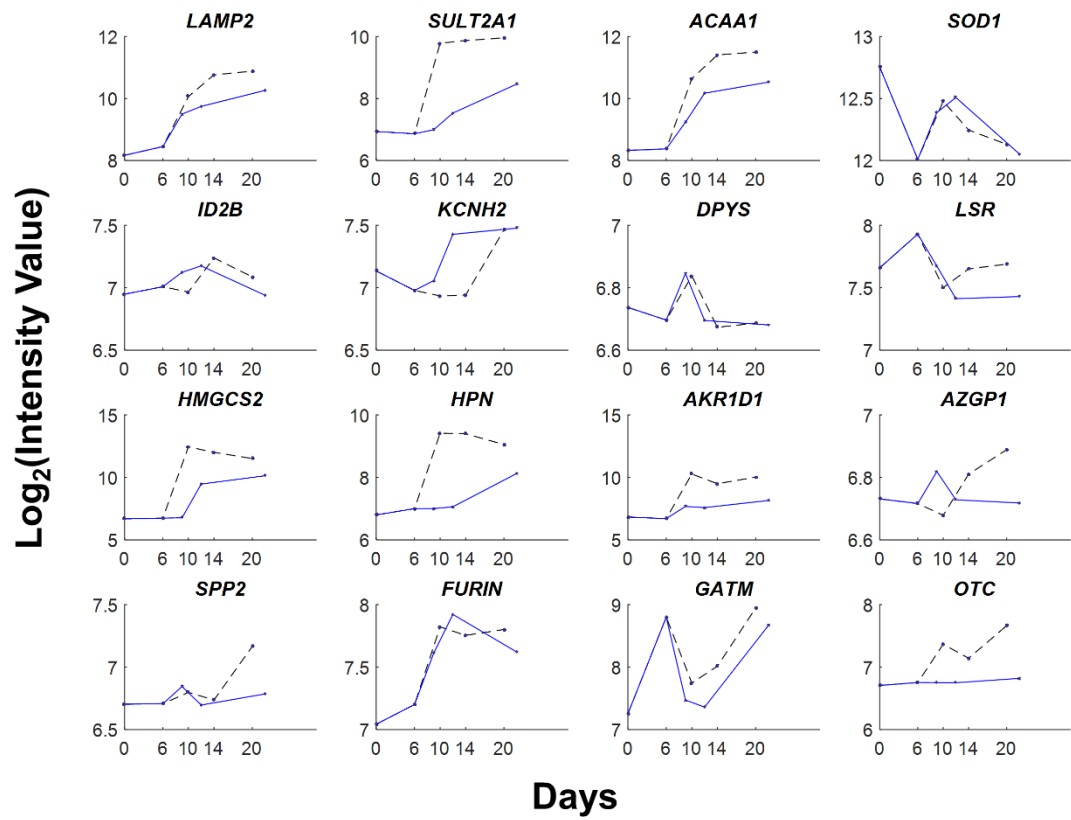


Liver Specific Genes



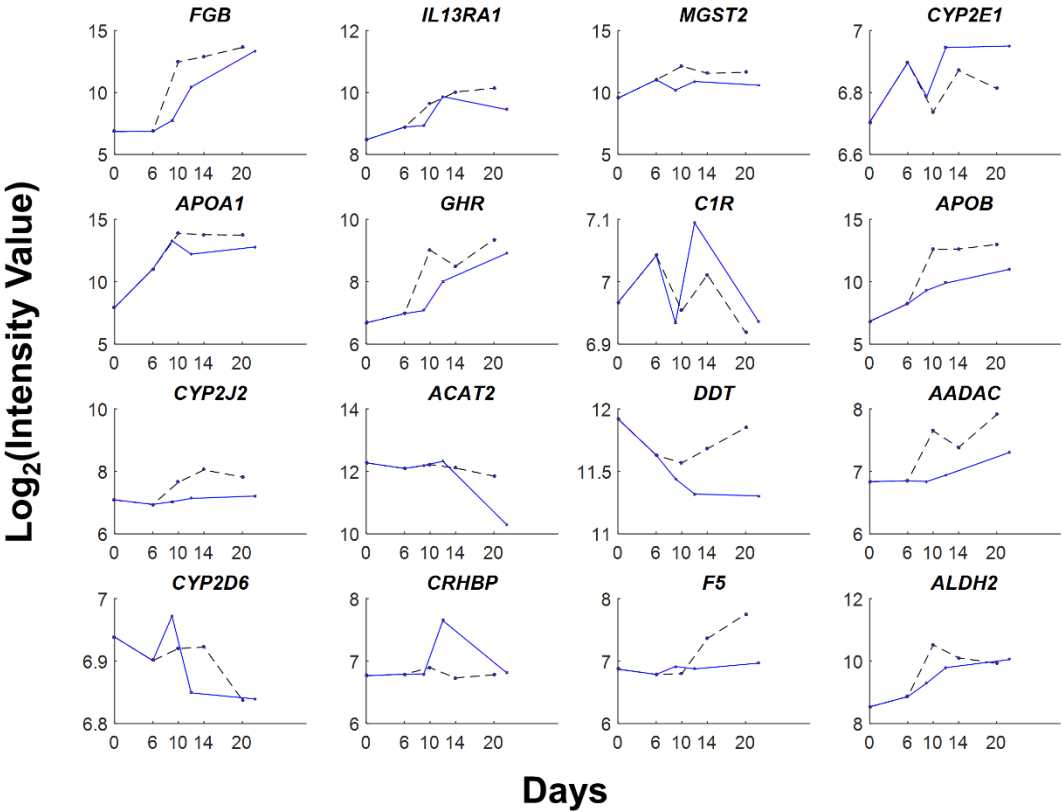
m

Liver Specific Genes



n

Liver Specific Genes



O

Liver Specific Genes

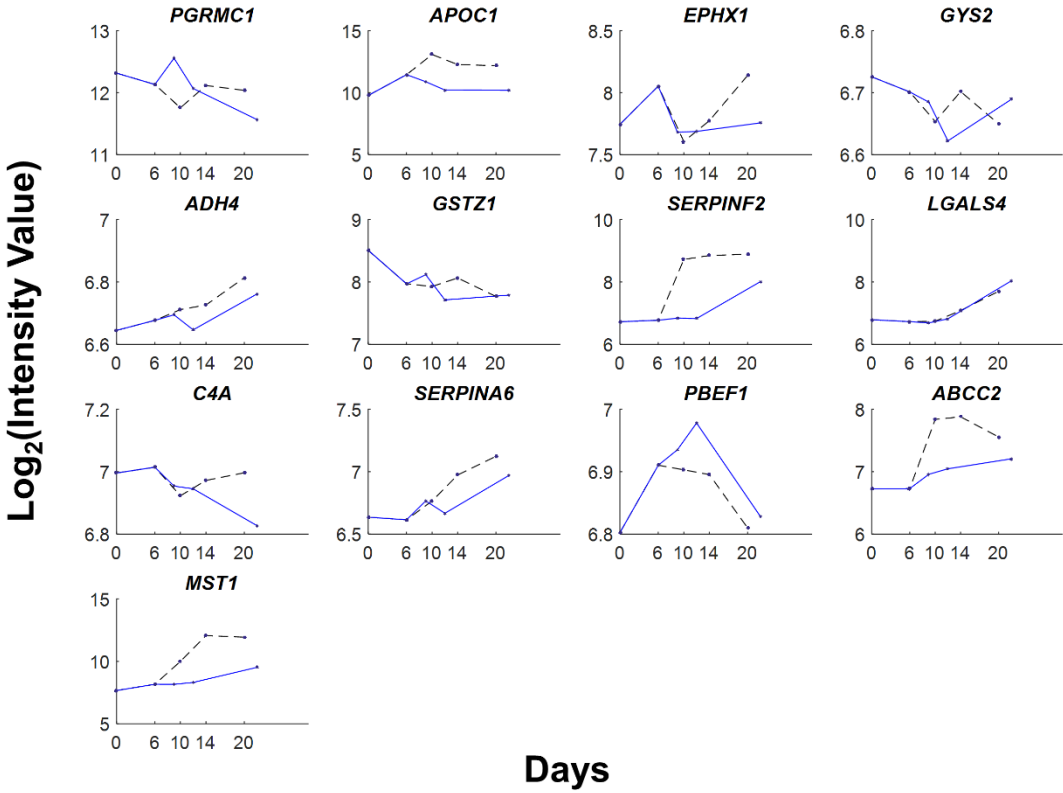


Figure S8a-o. Transcript dynamics of embryonic liver specific genes during directed differentiation with the original protocol or with simultaneous expansion.

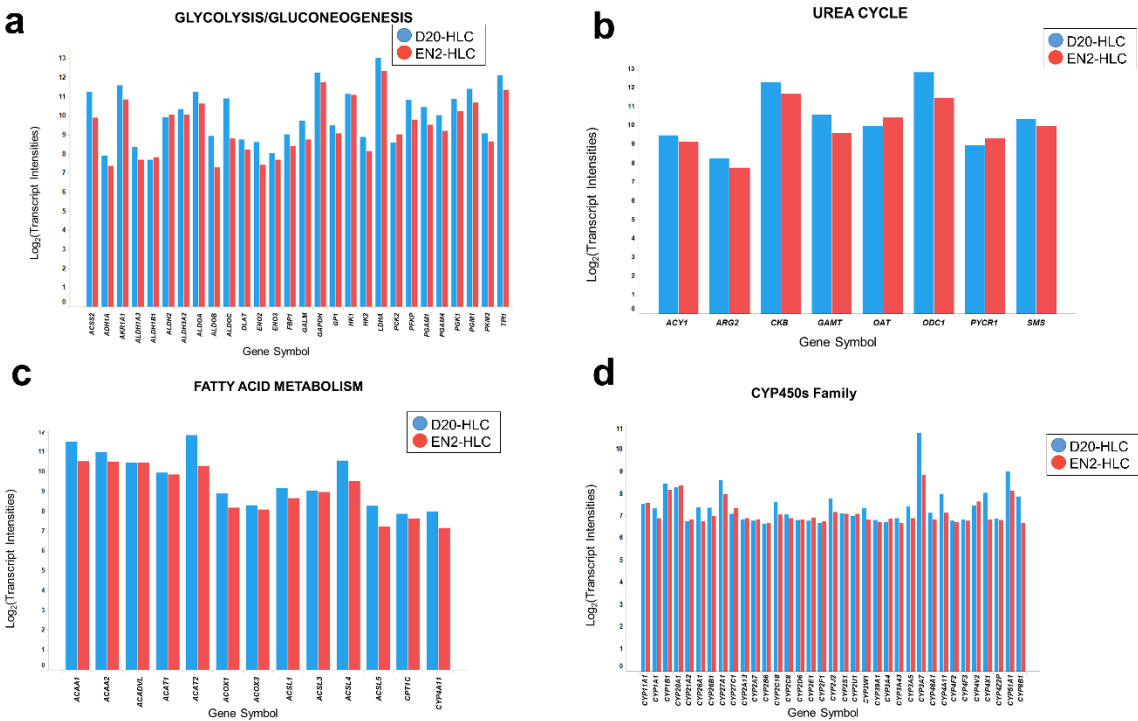


Figure S9. Comparison of transcript levels of genes of different functional classes between D20-HLC and EN2-HLC.

- (a) Expression levels of glycolysis/gluconeogenesis genes were similar between D20-HLCs and EN2-HLCs.
- (b) Expression levels of urea cycle genes were similar between D20-HLCs and EN2-HLCs.
- (c) Expression levels of fatty acid metabolism genes were similar between D20-HLCs and EN2-HLCs.
- (d) Expression levels of genes in the cytochrome p450 family were similar between D20-HLCs and EN2-HLCs.

Table S1: Primer list for qRT-PCR

Genes	Forward sequence	Reverse sequence
AAT	TTTAAAGGCAAATGGGAGAG	CCTAAACGCTTCATCATAGG
AFP	CCTACAATTCTTCTTTGGGCT	AGTAACAGTTATGGCTTGGA
ALB	TGGCACAATGAAGTGGGTAA	CTGAGCAAAGGCAATCAACA
CXCR4	AACTTCAGTTTGTGGCTGC	GAAACAGGGTTCCTTCATGG
CYP2A6	CAAAAAGGACACCAAGTTTCG	AGAGCCCAGCATAGGGTACA
CYP2C8	AAGAAAAGTGACTACTTCATGCCTTT	CAAGTCCTTCTCCTGCACAA
CYP2C9	ATTGACCTTCTCCCCACCA	CAGGGAAATTAATATGGTTGTGC
GAPDH	TGGTATCGTGGAAGGACTCATGAC	ATGCCAGTGAGCTTCCCGTTCAGC
GSC	TCTCAACCAGCTGCACTGTC	CCAGACCTCCACTTTCTCCTC
OCT4	GATGGCGTACTGTGGGCCC	TGGGACTCCTCCGGGTTTTG
PEPCK	AACGCCATGGCTACAATCC	AGGTAGCTCCGAATGTCACG